J|A|C|S
ARTICLES
Published on Web 03/13/2008

Organic n-Channel Transistors Based on Core-Cyanated Perylene Carboxylic Diimide Derivatives

R. Thomas Weitz,* Konstantin Amsharov, Ute Zschieschang, Esther Barrena Villas, Dipak K. Goswami, Marko Burghard, Helmut Dosch, Martin Jansen, Klaus Kern, and Hagen Klauk

Max Planck Institute for Solid State Research, Heisenbergstraβe 1, 70569 Stuttgart (Germany), Max Planck Institute for Metals Research, Heisenbergstraβe 3, 70569 Stuttgart (Germany), and Institut de Physique des Nanostructures, Ecole Polytechnique Fédérale de Lausanne, 1015 Lausanne (Switzerland)

Received June 26, 2007; E-mail: t.weitz@fkf.mpg.de

Abstract: Five core-cyanated perylene carboxylic diimides end-functionalized with fluorine-containing linear and cyclic substituents have been synthesized and employed in the fabrication of air-stable n-channel organic thin-film field-effect transistors with carrier mobilities up to 0.1 cm^2/Vs. The relationships between molecular structure, thin-film morphology, substrate temperature during vacuum deposition, transistor performance, and air stability have been investigated. Our experiments led us to conclude that the role of the fluorine functionalization in the air-stable n-channel operation of the transistors is different than previously thought.

Introduction

Organic semiconductors are in principle expected to show ambipolar transport characteristics[1] with both p-type and n-type conduction when employed as the active layer in a field-effect transistor (FET). In practice, the majority of the organic thin-film FETs reported to date show either p-type or n-type behavior, but not both. This phenomenon is actually advantageous for organic transistor applications, because ambipolar transport through the FET channel would lead to unacceptably large leakage currents, so that the transistor could not be completely turned off. (In silicon CMOS transistors, the semiconductor is ambipolar, but the leakage currents are very small (<1 pA) because the contacts are selectively doped p-type or n-type so that space−charge regions block undesired injection and leakage. For organic FETs, however, reliable contact doping has remained elusive.)

Several mechanisms are responsible for the often highly unbalanced characteristics of organic FETs. One is the fact that in most organic semiconductors the HOMO−LUMO gap is sufficiently large that only one of the two orbitals (usually the HOMO) is accessible for the efficient injection of charge carriers from the contacts. A second mechanism that promotes unbalanced transport is the selectivity of the deep trapping of injected carriers in the channel.[1] It appears that in many organic semiconductors negative charge carriers are trapped more efficiently than positive carriers, either at interfaces (such as the semiconductor/gate dielectric interface or at grain boundaries within the semiconductor) or by environmental traps (generated presumably by oxygen, water, or ozone). As a result, most organic FETs show p-channel behavior. The realization of many organic electronic applications, however, would benefit greatly from the availability of both n-channel FETs and p-channel FETs because this will allow the implementation of complementary circuits with low power consumption, high operation frequency, and sufficient robustness against device parameter variations and external noise.

A number of strategies have been developed to obtain organic FETs that operate as n-channel devices.[2] One is the use of a combination of organic semiconductor and electrode material for which electrons can be efficiently injected into the LUMO. This can be realized either by choosing a semiconductor with a large electron affinity or a contact metal with a low workfunction, or both. Another strategy is the elimination of electron traps from the transistor by passivating the dielectric interface and/or by operating the FET in an oxygen-free environment. Examples for the successful implementation of these two strategies include n-channel FETs based on C_{60} (refs 3 and 4] and on (hydrocarbon-functionalized) naphthalene or perylene carboxylic dianhydrides or diimides.[5−10] Other ex-

(1) Chua, L. L.; Zaumseil, J.; Chang, J. F.; Ou, E. C. W.; Ho, P. K. H.; Sirringhaus, H.; Friend, R. H.; General Observation of n-Type Field-Effect Behaviour in Organic Semiconductors. *Nature* **2005**, *434* (7030), 194−199.

(2) Facchetti, A. Semiconductors for Organic Transistors. *Mater. Today* **2007**, *10* (3), 28−37.

(3) Haddon, R. C.; Perel, A. S.; Morris, R. C.; Palstra, T. T. M.; Hebard, A. F.; Fleming, R. M. C-60 Thin-Film Transistors. *Appl. Phys. Lett.* **1995**, *67* (1), 121−123.

(4) Kobayashi, S.; Takenobu, T.; Mori, S.; Fujiwara, A.; Iwasa, Y. Fabrication and Characterization of C-60 Thin-Film Transistors with High Field-Effect Mobility. *Appl. Phys. Lett.* **2003**, *82* (25), 4581−4583.

(5) Horowitz, G.; Kouki, F.; Spearman, P.; Fichou, D.; Nogues, C.; Pan, X.; Garnier, F. Evidence for n-Type Conduction in a Perylene Tetracarboxylic Diimide Derivative. *Adv. Mater.* **1996**, *8* (3), 242-&.

(6) Laquindanum, J. G.; Katz, H. E.; Dodabalapur, A.; Lovinger, A. J. n-Channel Organic Transistor Materials Based on Naphthalene Frameworks. *J. Am. Chem. Soc.* **1996**, *118* (45), 11331−11332.

amples are n-channel FETs based on pentacene[11] and poly(9,9-dioctylfluorene) (ref 1) that employ low-workfunction metal contacts and a dielectric interface with a reduced density of active electron traps. Generally, all of these transistors operate properly only in a vacuum or in an inert atmosphere, apparently because certain species present in ambient air, such as oxygen, easily diffuse into the semiconductor and destabilize or trap the negative charge carriers in the channel. (This does not mean that the organic semiconductor is destroyed by oxygen exposure; devices typically recover upon returning to an inert ambient.)

A third strategy that has been developed and has led to the demonstration of organic n-channel FETs that can be operated in air is the functionalization of conjugated compounds with fluorine-rich substituents. This was first reported by Bao and co-workers for copper phthalocyanine (CuPc).[12] FETs based on CuPc only show p-channel operation, whereas FETs based on the perfluorinated counterpart, F_{16}CuPc, operate as n-channel FETs in air with a mobility of 0.03 cm^2/Vs and excellent long-term stability.[13,14]

This raises the question about the mechanism by which the fluorine-containing substituents promote air stability. Fluorine functionalization to create organic semiconductors for n-channel FETs works for other material systems as well, for example, for naphthalene carboxylic diimides,[15−17] perylene carboxylic diimides,[18,19] oligothiophenes,[20−26] and for pentacene.[27,28] However, although these materials have demonstrated n-channel FET operation, not all of them operate in air. It appears that fluorine functionalization generally helps in obtaining n-channel FETs but that it promotes air stability only for certain types of materials (such as $CH_2C_6H_4CF_3$-functionalized naphthalene carboxylic diimide FETs that show an n-channel mobility of 0.12 cm^2/Vs both in vacuum and in air[15]) but not for others (such as FETs based on perfluorinated pentacene[28] or fluoroalkyl-oligothiophenes[25]). The exact mechanism for this remains unclear, especially because in some cases fluorine functionalization appears to actually reduce the mobility. For example, FETs based on $CH_2(CF_2)_6CF_3$-substituted naphthalene carboxylic diimide have shown n-channel mobilities that are three times smaller than the n-channel mobilities of FETs based on the $(CH_2)_7CH_3$-substituted derivatives (~0.05 cm^2/Vs vs 0.16 cm^2/Vs, both measured in vacuum).[15]

Recently, Jones et al. synthesized two perylene carboxylic diimide derivatives with a cyano-functionalized perylene core and obtained n-channel FETs with excellent performance in air.[29] One of the compounds was end-functionalized with cyclohexane groups and showed a mobility of 0.1 cm^2/Vs, whereas the other was end-functionalized with fluoroalkyl substituents and exhibited a mobility of 0.6 cm^2/Vs. Apparently, functionalizing only the perylene core with strongly electron-withdrawing groups (e.g., cyano groups[29] or chlorine groups[30,31]) is sufficient to induce air stability, whereas the additional functionalization of the diimide groups with electron-withdrawing substituents promotes a further increase of the mobility in air. In the case of fluoroalkyl-substituted naphthalene and perylene carboxylic diimide derivatives, the observation of air stability has been attributed to the close packing of the

(7) Suga, T.; Iizuka, M.; Kuniyoshi, S.; Kudo, K.; Tanaka, K. Determination of Effects of Purity and Atmospheric Gases on Electrical Properties of Perylene Thin Films by Field Effect Measurement. *Synth. Met.* **1999**, *102* (1−3), 1050−1051.
(8) Malenfant, P. R. L.; Dimitrakopoulos, C. D.; Gelorme, J. D.; Kosbar, L. L.; Graham, T. O.; Curioni, A.; Andreoni, W. N-Type Organic Thin-Film Transistor with High Field-Effect Mobility Based on a *N,N′*-Dialkyl-3,4,9,-10-perylene Tetracarboxylic Diimide Derivative. *Appl. Phys. Lett.* **2002**, *80* (14), 2517−2519.
(9) Gundlach, D. J.; Pernstich, K. P.; Wilckens, G.; Gruter, M.; Haas, S.; Batlogg, B. High Mobility n-Channel Organic Thin-Film Transistors and Complementary Inverters. *J. Appl. Phys.* **2005**, 98 (6).
(10) Tatemichi, S.; Ichikawa, M.; Koyama, T.; Taniguchi, Y. High Mobility n-Type Thin-Film Transistors Based on *N,N′*-Ditridecyl Perylene Diimide with Thermal Treatments. *Appl. Phys. Lett.* **2006**, *89* (11).
(11) Ahles, M.; Schmechel, R.; von Seggern, H. n-Type Organic Field-Effect Transistor Based on Interface-Doped Pentacene. *Appl. Phys. Lett.* **2004**, *85* (19), 4499−4501.
(12) Bao, Z. A.; Lovinger, A. J.; Brown, J. New Air-Stable n-Channel Organic Thin Film Transistors. *J. Am. Chem. Soc.* **1998**, *120* (1), 207−208.
(13) Ling, M. M.; Bao, Z. N.; Erk, P. Air-Stable n-Channel Copper Hexachlorophthalocyanine for Field-Effect Transistors. *Appl. Phys. Lett.* **2006**, *89* (16).
(14) Klauk, H.; Zschieschang, U.; Pflaum, J.; Halik, M. Ultralow-Power Organic Complementary Circuits. *Nature* **2007**, *445* (7129), 745.
(15) Katz, H. E.; Johnson, J.; Lovinger, A. J.; Li, W. J. Naphthalenetetracarboxylic Diimide-Based n-Channel Transistor Semiconductors: Structural Variation and Thiol-Enhanced Gold Contacts. *J. Am. Chem. Soc.* **2000**, *122* (32), 7787−7792.
(16) Katz, H. E.; Lovinger, A. J.; Johnson, J.; Kloc, C.; Siegrist, T.; Li, W.; Lin, Y. Y.; Dodabalapur, A. A Soluble and Air-Stable Organic Semiconductor with High Electron Mobility. *Nature* **2000**, *404* (6777), 478−481.
(17) Kao, C. C.; Lin, P.; Lee, C. C.; Wang, Y. K.; Ho, J. C.; Shen, Y. Y. High-Performance Bottom-Contact Devices Based on an Air-Stable n-Type Organic Semiconductor *N,N*-bis(4-Trifluoromethoxybenzyl)-1,4,5,8-naphthalene-tetracarboxylic di-imide. *Appl. Phys. Lett.* **2007**, *90* (21).
(18) Chen, H. Z.; Ling, M. M.; Mo, X.; Shi, M. M.; Wang, M.; Bao, Z. Air Stable n-Channel Organic Semiconductors for Thin Film Transistors Based on Fluorinated Derivatives of Perylene Diimides. *Chem. Mater.* **2007**, *19* (4), 816−824.
(19) Hosoi, Y.; Tsunami, D.; Hisao, I.; Furukawa, Y. Air-Stable n-Channel Organic Field-Effect Transistors Based on N,N′-bis(4-Trifluoromethylbenzyl)perylene-3,4,9, 10-Tetracarboxylic Diimide. *Chem. Phys.* Letters **2007**, *436* (1−3), 139−143.
(20) Facchetti, A.; Deng, Y.; Wang, A. C.; Koide, Y.; Sirringhaus, H.; Marks, T. J.; Friend, R. H. Tuning the Semiconducting Properties of Sexithiophene by Alpha,Omega-Substitution - Alpha,Omega-Diperfluorohexylsexithiophene: The First n-Type Sexithiophene for Thin-Film Transistors. *Angew. Chem., Int. Ed.* **2000**, *39* (24), 4547.
(21) Facchetti, A.; Mushrush, M.; Katz, H. E.; Marks, T. J. n-Type Building Blocks for Organic Electronics: A Homologous Family of Fluorocarbon-Substituted Thiophene Oligomers with High Carrier Mobility. *Adv. Mater.* **2003**, *15* (1), 33-+.
(22) Facchetti, A.; Yoon, M. H.; Stern, C. L.; Katz, H. E.; Marks, T. J. Building Blocks for n-Type Organic Electronics: Regiochemically, Modulated Inversion of Majority Carrier Sign in Perfluoroarene-Modified Polythiophene Semiconductors. *Angew. Chem., Int. Ed.* **2003**, *42* (33), 3900−3903.
(23) Facchetti, A.; Letizia, J.; Yoon, M. H.; Mushrush, M.; Katz, H. E.; Marks, T. J. Synthesis and Characterization of Diperfluorooctyl-Substituted Phenylene-Thiophene Oligomers as n-Type Semiconductors. Molecular Structure-Film Microstructure-Mobility Relationships, Organic Field-Effect Transistors, and Transistor Nonvolatile Memory Elements. *Chem. Mater.* **2004**, *16* (23), 4715−4727.
(24) Facchetti, A.; Mushrush, M.; Yoon, M. H.; Hutchison, G. R.; Ratner, M. A.; Marks, T. J. Building Blocks for n-Type Molecular and Polymeric Electronics. Perfluoroalkyl versus Alkyl-Functionalized Oligothiophenes (nT; $n = 2-6$). Systematics of Thin Film Microstructure, Semiconductor Performance, and Modeling of Majority Charge Injection in Field-Effect Transistors. *J. Am. Chem. Soc.* **2004**, *126* (42), 13859−13874.
(25) Yoon, M. H.; Facchetti, A.; Stern, C. E.; Marks, T. J. Fluorocarbon-Modified Organic Semiconductors: Molecular Architecture, Electronic, and Crystal Structure Tuning of Arene-Versus Fluoroarene-Thiophene Oligomer Thin-Film Properties. *J. Am. Chem. Soc.* **2006**, *128* (17), 5792−5801.
(26) Yoon, M. H.; Kim, C.; Facchetti, A.; Marks, T. J. Gate Dielectric Chemical Structure-Organic Field-Effect Transistor Performance Correlations for Electron, Hole, and Ambipolar Organic Semiconductors. *J. Am. Chem. Soc.* **2006**, *128* (39), 12851−12869.
(27) Sakamoto, Y.; Suzuki, T.; Kobayashi, M.; Gao, Y.; Fukai, Y.; Inoue, Y.; Sato, F.; Tokito, S. Perfluoropentacene: High-Performance, p−n Junctions and Complementary Circuits with Pentacene. *J. Am. Chem. Soc.* **2004**, *126* (26), 8138−8140.
(28) Inoue, Y.; Sakamoto, Y.; Suzuki, T.; Kobayashi, M.; Gao, Y.; Tokito, S. Organic Thin-Film Transistors with High Electron Mobility Based on Perfluoropentacene. *Japanese Journal Of Applied Physics Part 1-Regular Papers Short Notes & Review Papers* **2005**, *44* (6A), 3663−3668.
(29) Jones, B. A.; Ahrens, M. J.; Yoon, M. H.; Facchetti, A.; Marks, T. J.; Wasielewski, M. R. High-Mobility Air-Stable n-Type Semiconductors with Processing Versatility: Dicyanoperylene-3,4: 9,10-bis(Dicarboximides). *Angew. Chem., Int. Ed.* **2004**, *43* (46), 6363−6366.
(30) Ling, M. M.; Erk, P.; Gomez, M.; Koenemann, M.; Locklin, J.; Bao, Z. N. Air-Stable n-Channel Organic Semiconductors Based on Perylene Diimide Derivatives without Strong Electron Withdrawing Groups. *Adv. Mater.* **2007**, *19* (8), 1123−1127.
(31) Ling, M. M.; Bao, Z.; Erk, P.; Koenemann, M.; Gomez, M. Complementary Inverter Using High Mobility Air-Stable Perylene Di-Imide Derivatives. *Appl. Phys. Lett.* **2007**, *90*, 093508.

Scheme 1. Organic Semiconductors Synthesized and Investigated in This Work.

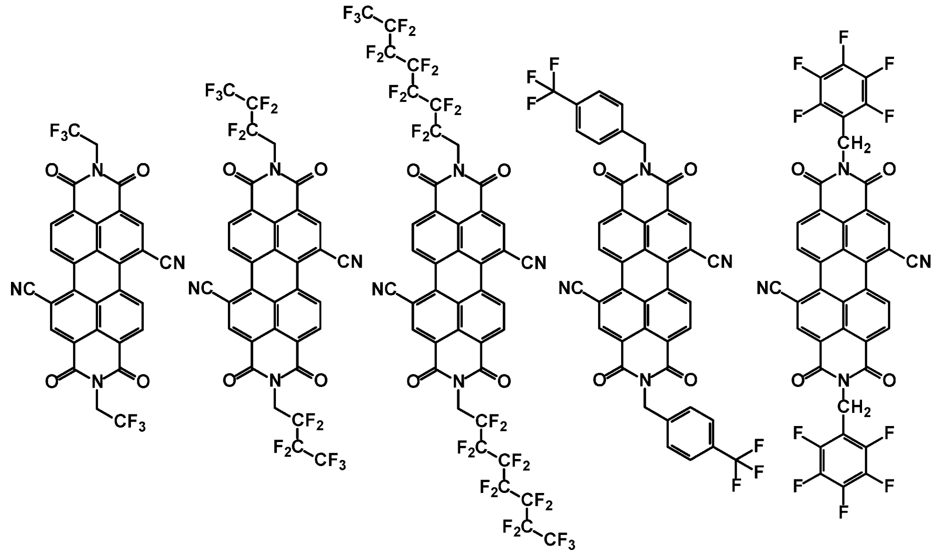

1 2 3 4 5

fluoroalkyl substituents. These functionalities are believed to act as a kinetic barrier against oxygen penetration into the film.[15,29]

With the intent of elucidating the role of the fluorine functionalities in the air stability of perylene derivatives, we have synthesized and characterized a series of core-cyanated perylene carboxylic diimides end-functionalized with more or less fluorine-rich and more or less bulky substituents. All five compounds show n-channel FET behavior in air, with mobilities that span several orders of magnitude, but all with a very similar rate of degradation in air.

Results and Discussion

The five compounds, shown in Scheme 1, were synthesized according to the general procedure described by Katz et al., Shi et al., and Jones et al.[15,29,32] **2** is the same as the one reported by Jones et al., whereas **1**, **3**, **4**, and **5** have to our knowledge not been previously reported. For structural and electrical characterization, 30 nm thick films of each compound were deposited by thermal evaporation in vacuum onto heavily doped, thermally oxidized, silicon substrates covered with a hydrophobic self-assembled monolayer of octadecyltrichlorosilane (OTS). Structural characterization of the organic films was performed by atomic force microscopy (AFM) and X-ray diffraction (XRD). Thin-film FETs were prepared by evaporating 30 nm thick gold source/drain contacts directly onto the organic films (Figure 3). All of the electrical measurements were performed in air at room temperature. The AFM and XRD data indicate that the film morphology depends strongly on the substrate temperature but also on the substituent.

We will first discuss the morphology of films prepared from **2** because this is the compound that has shown the largest carrier mobility. Films of **2** deposited onto substrates held at a temperature of 140 °C show the highest degree of molecular order, judging from the AFM data (part b of Figure 1). Large crystallites composed of flat terraces and abrupt steps as well as screw dislocations can be seen. For a discussion about the origin of the screw dislocations, please refer to Figure S1 (Supporting Information). Between the individual crystallites, areas of the substrate not covered with the deposited compound are clearly observed, suggesting that at this elevated temperature the material partially dewets the surface. The film appears to be composed of two polymorphs,[33] that is, two areas in which the molecules are arranged in different orientations. In part b of Figure 1, polymorph A is characterized by terraces with round edges, whereas in polymorph B one edge of each terrace is usually faceted. Under an optical microscope, the two polymorphs have different colors: A appears red, whereas B appears green. The formation of two polymorphs showing different molecular arrangements as well as colors has been previously reported for perylene[34] and perylene derivatives.[35,36] The different colors of the two polymorphs were attributed to excitonic effects.[35]

When **2** is deposited at substrate temperatures below 140 °C, the films are characterized by full surface coverage but appear less ordered; this can be seen in the AFM images of films deposited at 120 °C (part a of Figure 1) and 100, 80, and 25 °C (Figure S2 in the Supporting Information). In the AFM images of the films grown at 120 °C, only polymorph A is visible, that is, the islands are usually round (part a of Figure 1), and under an optical microscope they appear red. (Note that from the AFM data alone we cannot rule out that polymorph B also exists at 120 °C.) At deposition temperatures below 100 °C, the terraces are less pronounced, indicating that these films are even less ordered.

(32) Shi, M. M.; Chen, H. Z.; Sun, J. Z.; Ye, J.; Wang, M. Fluoroperylene Diimide: A Soluble and Air-Stable Electron Acceptor. *Chem. Commun.* **2003**, (14), 1710−1711.

(33) Threlfall, T. L. Analysis Of Organic Polymorphs - A Review. *Analyst* **1995**, *120* (10), 2435−2460.

(34) Tanaka, J. The Electronic Spectra Of Aromatic Molecular Crystals.2. The Crystal Structure And Spectra Of Perylene. *Bull. Chem. Soc. Jpn.* **1963**, *36* (10), 1237−1249.

(35) Mizuguchi, J.; Hino, K.; Tojo, K. Strikingly different electronic spectra of structurally similar perylene imide compounds. *Dyes Pigm.* **2006**, *70* (2), 126−135.

(36) Mobus, M.; Karl, N.; Kobayashi, T. Structure Of Perylene-Tetracarboxylic-Dianhydride Thin-Films On Alkali-Halide Crystal Substrates. *J. Cryst. Growth* **1992**, *116* (3−4), 495−504.

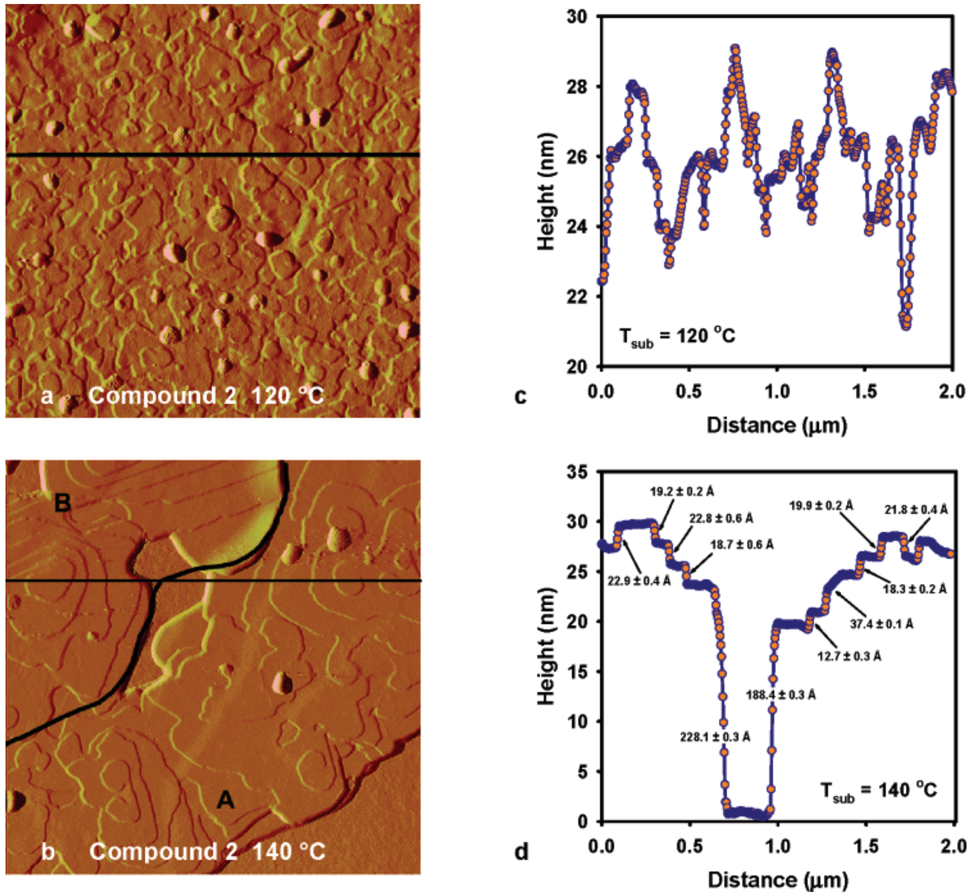

Figure 1. (a) Atomic force microscopy (AFM) amplitude image (size 2 × 2 μm^2) of a 30 nm thick film of **2** deposited at a substrate temperature of 120 °C. (b) AFM amplitude image of **2** deposited at a substrate temperature of 140 °C. In both images, islands with discrete steps and screw dislocations can be recognized. The boundary between polymorph A and B is marked by a black line for clarity. Panels (c) and (d) are linescans at the positions indicated by the black lines in (a) and (b).

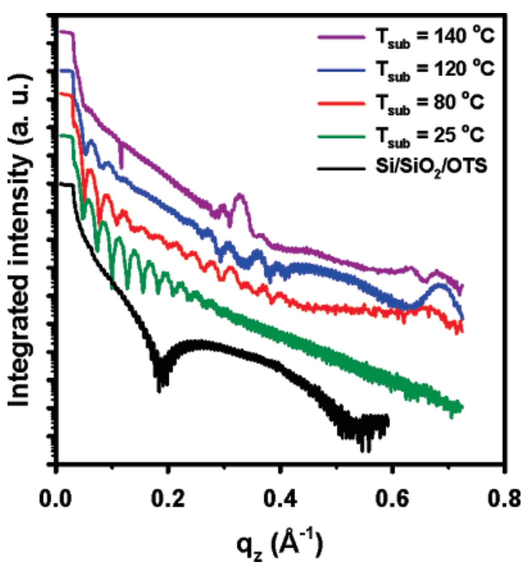

Figure 2. Specular X-ray diffraction data of the OTS-covered Si/SiO_2 substrate and of thin films of **2** deposited at different substrate temperatures. Note that increasing the deposition temperature leads to a roughening of the films due to the rough dewetting morphology. In films grown at 140 °C, the Kiessig oscillations are completely destroyed.

To gain further insight into the film structure at different temperatures and to elucidate the two polymorphs observed by AFM, we performed X-ray diffraction measurements on the films of **2**. Out-of-plane X-ray diffraction and grazing incidence X-ray diffraction (GIXD) measurements were performed on films deposited at 25, 80, 120, and 140 °C (Figure 2). The XRD data show that the films grown at 25 °C are completely amorphous as can be discerned from the absence of discrete Bragg peaks in the spectrum. Pronounced Kiessig oscillations arising from interference between the semiconductor film and the OTS interfaces show that the films deposited at this temperature are very smooth (with a mean square roughness of only 8.6 Å). Films grown at 80 °C display a small degree of short-range molecular order, and films grown at 120 and 140 °C are characterized by a large degree of crystalline molecular ordering.

For the films grown at 120 and 140 °C, the out-of-plane Bragg reflections display two distinct peaks; one peak is associated with a *d* spacing of 19.2 Å (q_z = 0.3279 $Å^{-1}$) and the other peak with a *d* spacing of 9.2 Å (q_z = 0.6834 $Å^{-1}$). The finding of two periodicities confirms that **2** crystallizes in two different polymorphs[33] characterized by different orientations of the molecules. The *d* spacing of 19.2 Å is similar to the step heights measured by AFM in both polymorphs (usually between 19 and 21 Å), whereas the *d* spacing of 9.2 Å is much smaller than the step heights measured by AFM. This apparent discrepancy can be explained by assuming that in polymorph A the molecules form layers with a thickness of two molecules. Thus, the observed *d* spacing of 9.2 Å would correspond to a step height of 18.4 Å (which is indeed similar to what we measured by AFM). In this picture, in polymorph A the molecules would be

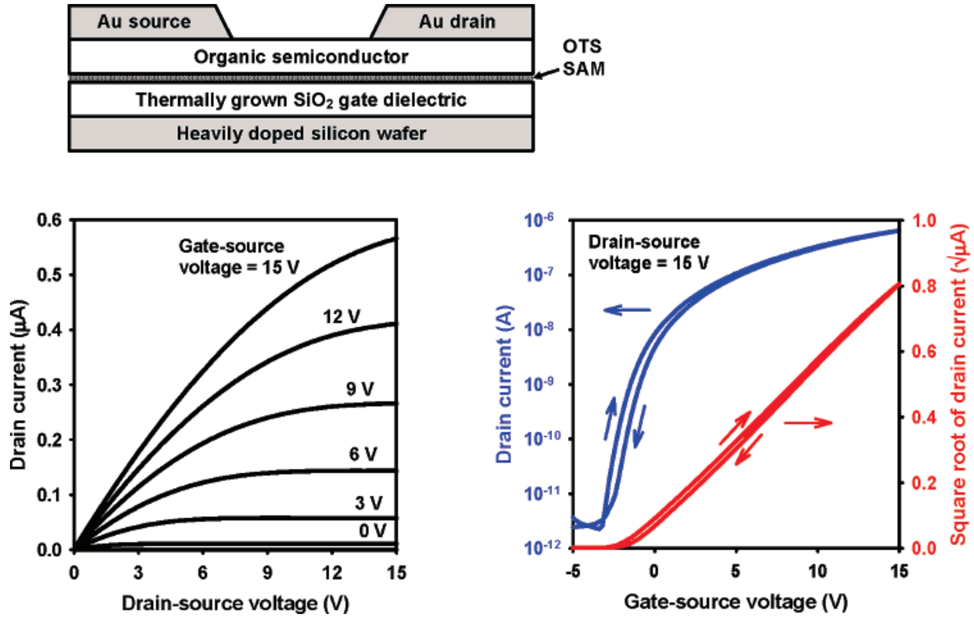

Figure 3. Cross section of the organic TFTs and output and transfer characteristics of a transistor based on **2** deposited at a substrate temperature of 120 °C. The transistor has a carrier mobility of 0.1 cm^2/Vs and a subthreshold swing of 0.5 V/decade.

oriented with their long axis parallel to the substrate; in polymorph B, however, they would be oriented with their long axis approximately upright on the substrate surface. In fact, in polymorph A (but not in polymorph B) we have occasionally found steps with a height significantly smaller than 19 Å (part d of Figure 1 and Figure S3 in the Supporting Information), which supports the existence of the two polymorphs. Judging from the relative intensity of the peaks found for the two periodicities, films deposited at a temperature of 120 °C seem to be predominantly composed of polymorph A.

The large degree of crystallinity and the presence of two different molecular orientations are also apparent from the GIXD data (Figure S4 in the Supporting Information). A detailed crystallographic study will be necessary to confirm the proposed molecular ordering of the two polymorphs. In both polymorphs, the molecular arrangement provides a favorable π overlap in the direction of the charge transport parallel to the substrate surface.

Compared with **2**, **1** has a shorter fluoroalkyl substituent, **3** has a longer fluoroalkyl substituent, and **4** and **5** have cyclic substituents. Of all five materials, **1** has by far the strongest tendency to dewet the surface. Disconnected islands are formed at substrate temperatures as low as 60 °C (Figure S5 in the Supporting Information). This is apparently a consequence of the shorter substituents. To obtain full surface coverage with **1**, the substrate temperature must be reduced to 25 °C, and at this temperature the films appear entirely disordered (Figure S6 in the Supporting Information).

3, on the other hand, requires higher substrate temperatures to create a high degree of molecular order. When deposited at a substrate temperature of 140 °C, crystallites with a step height of 28.5 ± 0.8 Å are seen in the AFM images (Figure S6 in the Supporting Information). Thus, the step height in films of **3** is larger by about 9 Å than the step height in polymorph A of **2**. From this we conclude that the molecules of **3** are not oriented in the same way as polymorph A of **2**, that is, not with their long axis parallel to the substrate. Instead, we believe the molecules of **3** stand with their long axis approximately upright on the substrate surface.

Table 1. Summary of the Electrical Characteristics of Organic Thin-Film Transistors Made Using Compounds **1** through **5**[a]

compound	T_{sub}	carrier mobility	threshold voltage	on/off ratio
1	25 °C	4·10^{-6} cm^2/Vs	~0 V	<10^1
	>60 °C	no field effect		
2	100 °C	0.06 cm^2/Vs	−2 V	10^5
	120 °C	**0.1 cm^2/Vs**	**−1 V**	**10^5**
	140 °C	0.009 cm^2/Vs	−1 V	10^5
3	120 °C	3·10^{-4} cm^2/Vs	−3 V	10^3
	140 °C	**0.05 cm^2/Vs**	**−1 V**	**10^5**
	160 °C	0.04 cm^2/Vs	1 V	10^5
4	**120 °C**	**0.004 cm^2/Vs**	**−32 V**	**10^4**
	140 °C	0.003 cm^2/Vs	−24 V	10^4
5	100 °C	7·10^{-6} cm^2/Vs	~0 V	10^1
	120 °C	**0.002 cm^2/Vs**	**−14 V**	**10^4**
	140 °C	no field effect		

[a] T_{sub} denotes the temperature of the substrate during the vacuum deposition of the organic semiconductor. The optimum deposition temperature for each compound is indicated in bold face.

When deposited at a substrate temperature of 140 °C, **4** forms closed layers with discrete steps, whereas **5** grows in disconnected islands. At a substrate temperature of 120 °C, both **4** and **5** form closed layers, although the films appear less ordered (Figure S6 in the Supporting Information).

FETs based on all five compounds were manufactured using the device structure shown in Figure 3. All of the transistors show exclusively n-channel characteristics and can be operated in air (Figure 3). The key device parameters are summarized in Table 1. The best performance was obtained with **2** deposited at a substrate temperature of 120 °C. This transistor has a carrier mobility of 0.1 cm^2/Vs, a threshold voltage of −1 V, a subthreshold swing of 0.5 V/decade, and an on/off current ratio of 10^5. The mobility is lower than the mobility reported by Jones et al. for the same compound, but this may be related to the lower operating voltage used in our experiments (15 V, instead of 100 V) and the different surface functionalization (OTS instead of HMDS). There is very little hysteresis in the transfer characteristics (Figure 3), and the subthreshold swing of 0.5

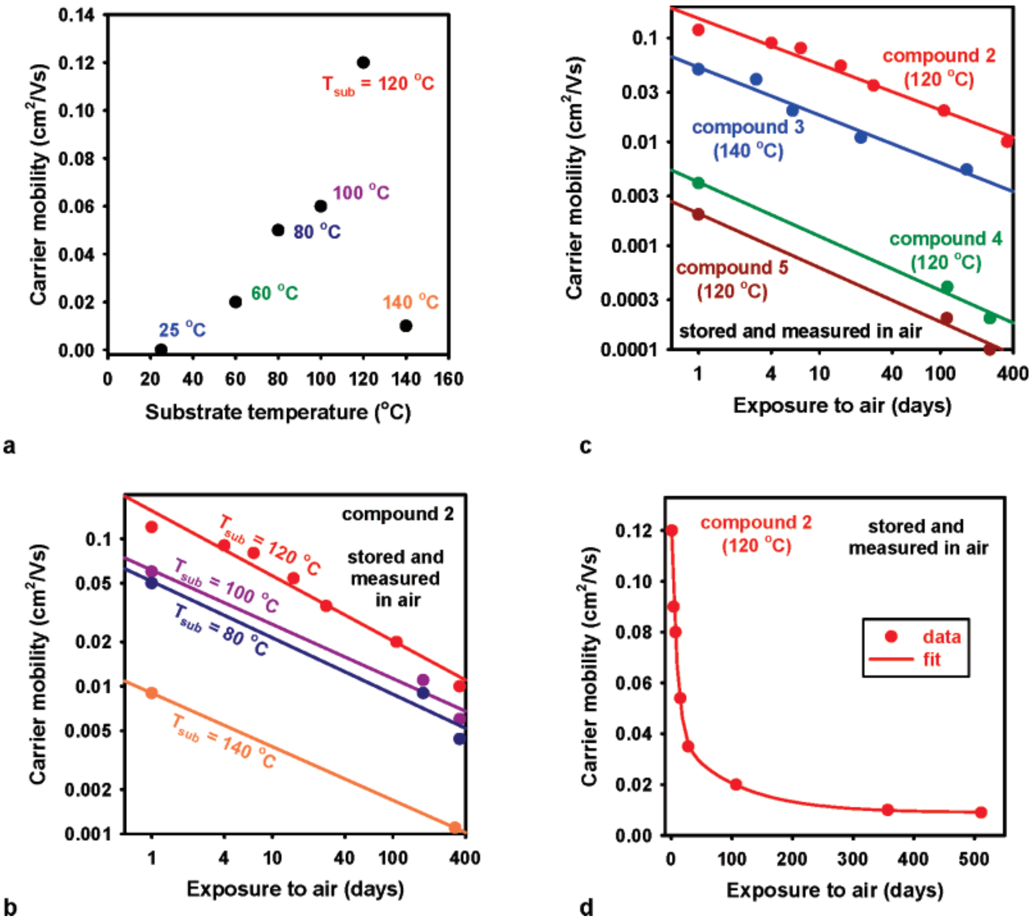

Figure 4. (a) Carrier mobilities of transistors based on **2** fabricated at different substrate temperatures. (b) Time-dependent degradation of the carrier mobility of FETs based on **2** deposited at different substrate temperatures. (c) Time-dependent degradation of the mobility of FETs based on **2**−**5**, each deposited at the optimum substrate temperature (**2**, 120 °C; **3**, 140 °C; **4**, 120 °C; **5**, 120 °C). The rate of degradation of the carrier mobility is similar for all of the FETs. The solid lines in (b) and (c) are a guide to the eye. (d) Exponential fit to the degradation data measured for **2** deposited at a substrate temperature of 120 °C.

V/decade is quite good for an organic FET. The carrier mobility of the FETs based on **2** increases almost monotonically over 4 orders of magnitude as the substrate temperature during the deposition is increased from 25 to 120 °C (part a of Figure 4). This agrees well with the AFM (Figure 1 and Figure S2 in the Supporting Information) and XRD (Figure 2) results, which suggest an increasing degree of molecular order with increasing substrate temperature. FETs prepared at a substrate temperature of 140 °C; however, have a much smaller drain current than FETs prepared at 120 °C, even though the XRD (Figure 2) data clearly show a higher degree of molecular order. The reason for the reduced drain current at 140 °C is that the material partially dewets the surface, so that the film is not completely closed at 140 °C. As a result, the FET transconductance has a maximum for a substrate temperature of 120 °C.

For FETs based on **1**, the performance (Table 1) peaks at a much lower substrate temperature (25 °C), apparently because the short substituents lead to distinct island growth at temperatures as low as 60 °C. However, at a substrate temperature of 25 °C the degree of molecular order in the film is very small, which explains the poor mobility (4×10^{-6} cm^2/Vs, similar to the mobility of **2** at this substrate temperature).

3 has a longer substituent than **2**, and consequently the transistor performance peaks at a higher substrate temperature (140 °C). FETs based on **3** prepared at 140 °C have relatively good performance (threshold voltage −1 V, subthreshold swing 1.2 V/decade, on/off ratio 10^5, small hysteresis), although the mobility is only half of the maximum mobility of **2** (0.05 cm^2/Vs, Figure S7 in the Supporting information and Table 1).

The two compounds with cyclic endgroups have a maximum mobility of 0.004 cm^2/Vs (**4**) and 0.002 cm^2/Vs (**5**), both for a substrate temperature of 120 °C (Table 1 and Figures S8 and S9 in the Supporting Information). The reason for the much lower mobilities in these two compounds is unclear but it is interesting that the FETs based on **4** and **5** also show a much more negative threshold voltage than the FETs based on the compounds with linear endgroups. This might suggest that the bulkier cyclic endgroups lead to a different crystal packing that is characterized both by a smaller degree of orbital overlap in the direction of transport in the channel (leading to a poor mobility) and by a greater density of defects (leading to a larger threshold voltage).

However, this interpretation is challenged by the recent results of Chen and co-workers,[18] who have observed mobilities as large as 0.06 cm^2/Vs for FETs based on perylene carboxylic diimides end-functionalized with bulky fluorine-rich cyclic endgroups. On the other hand, their compounds were not core-cyanated, so a direct comparison is difficult.

We also investigated the shelf life of the FETs prepared from **2** through **5** when stored under ambient conditions. Interestingly, all of the devices show about the same rate of mobility degradation in air (parts b and c of Figure 4). This observation is somewhat surprising because the molecules have different functional groups and the degree of order and the molecular orientation of both the functional groups as well as the perylene core in the films is expected to be quite different: for example, films of **2** prepared at 120 °C and **3** prepared at 140 °C are both characterized by a high degree of molecular order. In contrast, **2** prepared at 80 °C and **4** and **5** prepared at 120 °C appear much less ordered. Furthermore, in films of **2** prepared at 120 °C the molecules are oriented mainly with their long axis parallel to the substrate surface (polymorph A), so that the conjugated core of the molecule is exposed to the ambient and the film is therefore not protected from the ambient by the fluoroalkyl chains. In contrast, in films of **3** prepared at 140 °C the molecules stand with their long axis approximately upright on the substrate surface. Finally, the fluorinated functional groups vary in length and bulkiness (fluorinated alkyl chain of different length in **1** through **3**, cyclic substitutes in **4** and **5**), and thus the packing of the functional groups is expected to vary. Yet, all of the FETs show about the same rate of degradation. To rule out that the degradation of the mobility is caused by a macroscopic rearrangement of the organic molecules, we have performed AFM measurements of the films before and during the degradation investigations and found no apparent change in the film morphology.

We also note that the rate of mobility degradation is independent of the number of polymorphs in the film. Specifically, the FET in which the film is composed of two polymorphs (**2** deposited at a substrate temperature of 140 °C) shows the same rate of mobility degradation as the FETs in which the films are composed of only one polymorph (all other FETs).

The observation that **2**−**5** show the same rate of mobility degradation when stored under ambient conditions contradicts the hypothesis that densely packed fluorinated substituents form a kinetic barrier against the undesirable diffusion of environmental species (such as oxygen) into the semiconductor film.[29] If this hypothesis were correct, we would expect the films of **3** prepared at 140 °C to be more stable than the others because in films of **3** the molecules stand with their long axis upright on the substrate, so that the long and fluorine-rich $CH_2(CF_2)_6CF_3$ substituents are pointing toward the air. In contrast, FETs composed of **2** prepared at 120 °C should be less stable because in these films (mostly polymorph A) the fluoroalkyl chains do not protect the perylene cores from ambient species.

Furthermore, if the fluoroalkyl chains would form a kinetic barrier against the penetration of ambient species, the degradation of the FETs should also depend on the surface area exposed to the ambient: the larger the surface area, the larger the amount of ambient species able to penetrate into the film, and the faster the film would be expected to degrade. In addition to the surface area, the density of grain boundaries would then also be expected to influence the air stability of the FETs because grain boundaries are likely to enhance the diffusion of environmental traps into the film. In our FETs, however, we see neither an influence of the density of grain boundaries nor an effect of the surface area on the rate of mobility degradation: in films of **2** and **3**, which show a high degree of molecular order, both the surface area and the density of grain boundaries are larger compared to the less-ordered films of **4** and **5**. Yet, the rate of mobility degradation in air is similar for all of the compounds. Finally, if the hypothesis that a kinetic barrier is responsible for the air stability of the mobility was true,[15,29] different rates of mobility degradation would be expected depending on whether the film is continuous or not. However, in our experiments we find the same rate of mobility degradation for films with excellent surface coverage (**2** deposited at substrate temperatures of 80 to 120 °C and all films of **3**−**5**) and for films that are not continuous and partially dewet the surface (**2** deposited at a substrate temperature of 140 °C).

Another hypothesis is that the stability of charge carriers injected into the semiconductor film with respect to water and oxygen depends on the redox potential of the organic molecules. This hypothesis is based on observations on the stability of electron-conducting doped polymers.[37] Specifically, it has been hypothesized that FETs based on compounds with a redox potential smaller than that of oxygen can be operated in air only if the molecules are protected from oxygen by a kinetic barrier formed by densely packed fluorine-rich substituents. Jones et al. have reported that on the basis of its redox potential **2** would not be expected to be stable in air (unless the molecules are protected from oxygen).[29] However, as we have shown, our FETs can be operated in air independent of the possible presence of a kinetic barrier because we have observed the same rate of degradation for all of the compounds, regardless of the degree of molecular order and molecular orientation. Therefore, a mechanism unrelated to both the redox potential and the presence of a kinetic barrier appears to be responsible for the air stability of the n-channel organic semiconductors investigated in this work.

To gain further insight into the mechanism of the degradation of the mobility, it is viable to fit the time evolution of the mobility to a decay law. The degradation of the mobility in air over time is expected to follow an exponential law: $\mu(t) = \mu_0 e^{-t/\tau}$. However, if the mobility decay of **2** deposited at a substrate temperature of 120 °C (for which the most data points were collected) is fit to the equation $\mu(t) = \mu_0 e^{-t/\tau}$, the quality of the fit is not satisfactory ($\chi^2 = 3 \times 10^{-5}$). On the other hand, the agreement between data and model is better ($\chi^2 = 1 \times 10^{-5}$) if two consecutive degradation processes with different decay rates are considered:[38] $\mu(t) = \mu_1 e^{-t/\tau 1} + \mu_2 e^{-t/\tau\ 2} + C$. The fit yields $\tau_1 = 9$ days, $\tau_2 = 100$ days, $\mu_1 = 0.09$ cm^2/Vs, $\mu_2 = 0.03$ cm^2/Vs, and $C = 0.009$ cm^2/Vs. A possible explanation for the observation of two consecutive degradation processes is a decay process that proceeds from an initial state via an intermediate state to a final state. The future elucidation of the exact physical or chemical mechanisms behind this two-step decay process may provide further insight into the degradation processes of organic semiconductors.

Conclusions

In summary, we have investigated five organic semiconductors for use in n-channel field-effect transistors. Films of all of the compounds were vacuum-deposited at different substrate temperatures to study the evolution of the film morphology and to identify the best process conditions for optimum FET performance. The degree of molecular order in the films

(37) deLeeuw, D. M.; Simenon, M. M. J.; Brown, A. R.; Einerhand, R. E. F. Stability of n-Type Doped Conducting Polymers and Consequences for Polymeric Microelectronic Devices. *Synth. Met.* **1997**, *87* (1), 53−59.
(38) Atkins, P.; de Paula, J. *Atkins' Physical Chemistry*, 7th ed.; Oxford University Press: U.K., 2002.

increases with increasing deposition temperature up to a material-dependent temperature above which the molecules dewet the surface. FETs prepared from **2** deposited at a substrate temperature of 120 °C show the best electrical characteristics. They exhibit a carrier mobility of 0.1 cm^2/Vs, a subthreshold swing of 0.5 V/decade, and an on/off current ratio of 10^5. For lower substrate temperatures, the films are less ordered and the carrier mobility is lower, whereas the rate of mobility degradation in air is independent of the degree of molecular order in the film. In fact, the rate at which the mobility degrades in air is similar for all of the compounds and for all of the substrate temperatures. This demonstrates that the air stability cannot be easily explained by a assuming a kinetic barrier formed by densely packed fluorine substituents.

Materials and Methods

Materials. LDI-TOF mass spectra were obtained in a reflection mode on a Reflex IV (337 nm nitrogen laser) from Bruker Daltonik GmbH, Bremen, Germany. ^{1}H NMR spectra were recorded on a Bruker Avance 300 MHz spectrometer. Chemical shifts are expressed in ppm relative to the internal standard Me_4Si (δ 0.00). All of the reagents were purchased from Aldrich and ABCR and used as received. 1,7-dibromoperylene-3,4,9,10-tetracarboxydianhydride was obtained by bromination of perylene-3,4,9,10-tetracarboxydianhydride in concentrated sulfuric acid as described elsewhere.[29] Pentafluorobenzylamine was obtained by reduction of the corresponding benzonitrile according to the known procedure.[39] **1**−**5** were synthesized from 1,7-dibromoperylene-3,4,9,10-tetracarboxydianhydride in accordance to the same synthetic route as described for **2** (ref 29) (Scheme S1 in the Supporting Information). All of the compounds were purified via column flash chromatography on silica and characterized by ^{1}H NMR and LDI-TOF mass spectrometry. The NMR spectra showed the presence of small amounts of 1,6-isomers (1,6-dicyanoperylene) for all of the dicyano derivatives.

***N,N′*-bis(2,2,2-Trifluoroethyl)-1,7-dibromo-perylene-3,4:9,10−bis(dicarboximide) (1a).** Red solid (62% yield), R_f = 0.50 (DCM: Acetone 100:1); ^{1}H NMR ($CDCl_3$) δ 9.523 (d, J = 8.14 Hz, 2H), 8.984 (s, 2H), 8.75−8.80 (m, 2H), 4.95−5.10 (m, 4H); LDI-TOF MS Calcd for $C_{28}H_{10}Br_2F_6N_2O_4$ (M^-) 709.89, Found 709.72.

***N,N′*-bis(2,2,2-Trifluoroethyl)-1,7-dicyano-perylene-3,4:9,10−bis-(dicarboximide) (1b).** Red solid (71% yield), R_f = 0.28 (DCM:Acetone 100:2); ^{1}H NMR ($C_2D_2CL_4$) δ 9.02−9.05 (m, 2H), δ 8.26 (d, J = 8.17 Hz, 2H), δ 8.20−8.29 (m, 2H), δ 4.25−4.31 (m, 4H); LDI-TOF MS Calcd for $C_{30}H_{10}F_6N_4O_4$ (M^-) 604.06, Found 603.87.

***N,N′*-bis(1H,1H-Perfluorobutyl)-1,7-dibromo-perylene-3,4:9,10−bis(dicarboximide) (2a).** Red solid (82% yield), R_f = 0.67 (DCM: Acetone 100:2); ^{1}H NMR ($CDCl_3$) δ 9.506 (d, J = 8.16 Hz, 2H), 8.967 (s, 1H), 8.743 (d, J = 8.16 Hz, 2H), 5.017 (t, J = 15.36 Hz, 4H); LDI-TOF MS Calcd for $C_{32}H_{10}Br_2F_{14}N_2O_4$ (M^-) 909.88, Found 909.76.

***N,N′*-bis(1H,1H-Perfluorobutyl)-1,7-dicyano-perylene-3,4:9,10−bis(dicarboximide) (2b).** Red solid (76% yield), R_f = 0.32 (DCM: Acetone 100:2); ^{1}H NMR ($CDCl_3$) δ 9.728 (d, J = 8.23 Hz, 2H), 8.87−9.07 (m, 3H), 5.028 (t, J = 15.21 Hz, 4H); LDI-TOF MS Calcd for $C_{34}H_{10}F_{14}N_4O_4$ (M^-) 804.05, Found 804.22.

***N,N′*-bis(1H,1H-Perfluorooctyl)-1,7-dibromo-perylene-3,4:9,10−bis(dicarboximide) (3a).** Red solid (80% yield), R_f = 0.56 (DCM: Acetone 100:2); ^{1}H NMR ($CDCl_3$) δ 9.819 (d, J = 8.16 Hz, 2H), 8.948 (s, 1H), 8.750 (d, J = 8.16 Hz, 2H), 5.027 (t, J = 15.35 Hz, 4H); LDI-TOF MS Calcd for $C_{40}H_{10}Br_2F_{30}N_2O_4$ (M^-) 1309.85, Found 1309.73.

***N,N′*-bis(1H,1H-Perfluorooctyl)-1,7-dicyano-perylene-3,4:9,10−bis(dicarboximide) (3b).** Red solid (68% yield), R_f = 0.25 (DCM: Acetone 100:2); ^{1}H NMR ($CDCl_3$) δ 9.729 (d, J = 8.16 Hz, 2H), 9.032 (s, 1H), 8.986 (d, J = 8.16 Hz, 2H), 5.038 (t, J = 15.38 Hz, 4H); LDI-TOF MS Calcd for $C_{42}H_{10}F_{30}N_4O_4$ (M^-) 1204.02, Found 1203.91.

***N,N′*-bis(4-(Trifluoromethyl)benzyl)-1,7-dibromo-perylene-3,4:9,-10−bis(dicarboximide) (4a).** Red solid (76% yield), R_f = 0.41 (DCM: Acetone 100:2); ^{1}H NMR ($CDCl_3$) δ 9.476 (d, J = 8.16 Hz, 2H), 8.936 (s, 2H), 8.714 (d, J = 8.16 Hz, 2H), 7.549−7.663 (m, 8H), 5.432 (s, 4H); LDI-TOF MS Calcd for $C_{40}H_{18}Br_2F_6N_2O_4$ (M^-) 861.95, Found 861.62.

***N,N′*-bis(4-(Trifluoromethyl)benzyl)-1,7-dicyano-perylene-3,4:9,-10−bis(dicarboximide) (4b).** Red solid (43% yield), R_f = 0.24 (DCM: Acetone 100:2); ^{1}H NMR ($C_2D_2Cl_4$) δ 8.98 (d, J = 8.16 Hz, 2H), δ 8.25−8.36 (m, 4H), δ 6.95−7.01 (m, 8H), δ 4.78 (s, 4H); LDI-TOF MS Calcd for $C_{42}H_{18}F_6N_4O_4$ (M^-) 756.12, Found 755.98.

***N,N′*-bis(2,3,4,5,6-Pentafluorobenzyl)-1,7-dibromo-perylene-3,4:9,10−bis(dicarboximide) (5a).** Red solid (85% yield), R_f = 0.83 (DCM:Acetone 100:2); ^{1}H NMR ($CDCl_3$) δ 9.46−9.51 (m, 2H), 8.933 (dd, J = 4.78 Hz, 1.16 Hz, 2H), 8.68−8.73 (m, 2H), 5.468 (d, J = 26.37 Hz, 4H); LDI-TOF MS Calcd for $C_{38}H_{10}Br_2F_{10}N_2O_4$ (M^-) 905.88, Found 905.53.

***N,N′*-bis(2,3,4,5,6-Pentafluorobenzyl)-1,7-dicyano-perylene-3,4:9,10−bis(dicarboximide) (5b).** Red solid (88% yield), R_f = 0.48 (DCM:Acetone 100:2); ^{1}H NMR ($C_2D_2Cl_4$) δ 8.81−8.96 (m,2H), δ 8.21−8.33 (m,4H), δ 4.61−4.73 (m, 4H) LDI-TOF MS Calcd for $C_{40}H_{10}F_{10}N_4O_4$ (M^-) 800.05, Found 799.95.

Diffraction Experiments. The X-ray diffraction measurements were carried out at the Max Planck Institute for Metals Research's beamline at the Synchrotron Radiation Source ANKA in Karlsruhe, Germany, at a beam energy of 10 keV (λ = 1.23984 Å). The GIXD experiment was performed with the angles of the incident and exit X-ray beam close to the critical angle of the substrate α_{crit} = 0.1725°. The fit of the X-ray specular data was performed with the *Parratt32* software based on the Parratt algorithm.

Electrical Measurements. Heavily boron-doped and thermally oxidized silicon wafers were used as the substrate and gate electrode. The 100 nm thick SiO_2 gate oxide was functionalized with octadecyltrichlorosilane (OTS). The OTS self-assembles from the vapor phase in a low-pressure nitrogen atmosphere at a temperature of 150 °C, giving static contact angles between 100 and 105°. Organic semiconductors were evaporated at a rate of about 1 nm/min at a base pressure of about 10^{-6} mbar. During the deposition, the substrate was held at a constant temperature of 25, 60, 80, 100, 120, 140, or 160 °C. Thick gold source (30 nm) and drain contacts were evaporated through a shadow mask. All of the measurements were performed at room temperature in air on a Micromanipulator probe station with an Agilent 4156C Semiconductor Parameter Analyzer without specifically protecting the devices from the yellow laboratory light. Between electrical measurements, devices were stored in ambient air under (weak) yellow laboratory light. The carrier mobility (μ) was calculated from the I_D versus V_{GS} data in the saturation regime using the standard formula for field effect-transistors: $\mu = 2L/(WC_{ox})(dI_D/dV_{GS})^2$, where L is the channel length (130 μm), W is the channel width (170 μm), C_{ox} is the gate dielectric capacitance (35 nF/cm^2), I_D is the drain current, and V_{GS} is the gate-source voltage.

Acknowledgment. The TOC image was prepared using the software by Horcas et al.[40]

Supporting Information Available: AFM images of islands of **2**; AFM images of **1**−**5** deposited at different substrate

(39) Das, B. K.; Shibata, N.; Takeuchi, Y. Design and Synthesis of N-Nonpolar Nucleobase Dipeptides: Application of the Ugi Reaction for the Preparation of Dipeptides Having Uoroarylalkyl Groups Appended to the Nitrogen Atom. *J. Chem. Soc., Perkin Trans. 1* **2002**, (2), 197−206.

(40) Horcas, I.; Fernandez, R.; Gomez-Rodriguez, J. M.; Colchero, J.; Gomez-Herrero, J.; Baro, A. M. WSXM: A Software for Scanning Probe Microscopy and a Tool for Nanotechnology. *Rev. Sci. Instrum.* **2007**, 78, (1).

temperatures; a rocking curve and grazing incidence X-ray diffraction data from **2** deposited at different substrate temperatures; transfer and output curves of thin-film FETs based on **3**−**5**; a scheme of the synthesis route for **1**−**5**. Measured NMR and LDI-TOF MS spectra and calculated MS spectra of all of the compounds synthesized in this work. This material is available free of charge via the Internet at http://pubs.acs.org.

JA074675E

Supporting Information for

Organic n-Channel Transistors Based on Core-Cyanated Perylene Carboxylic Diimide Derivatives

R. Thomas Weitz,* Konstantin Amsharov, Ute Zschieschang, Esther Barrena Villas, Dipak K. Goswami, Marko Burghard, Helmut Dosch, Martin Jansen, Klaus Kern, **and** Hagen Klauk

R. T. Weitz, Dr. K. Amsharov, Dr. U. Zschieschang, Dr. M. Burghard, Prof. Dr. M. Jansen,

Prof. Dr. K. Kern, Dr. H. Klauk

E-mail: t.weitz@fkf.mpg.de

Max Planck Institute for Solid State Research Heisenbergstraße 1, 70569 Stuttgart (Germany)

Dr. E. Barrena Villas, Dr. D. K. Goswami, Prof. Dr. H. Dosch

Max Planck Institute for Metals Research

Heisenbergstraße 3, 70569 Stuttgart (Germany)

Prof. Dr. K. Kern

Institut de Physique des Nanostructures

Ecole Polytechnique Fédérale de Lausanne

1015 Lausanne (Switzerland)

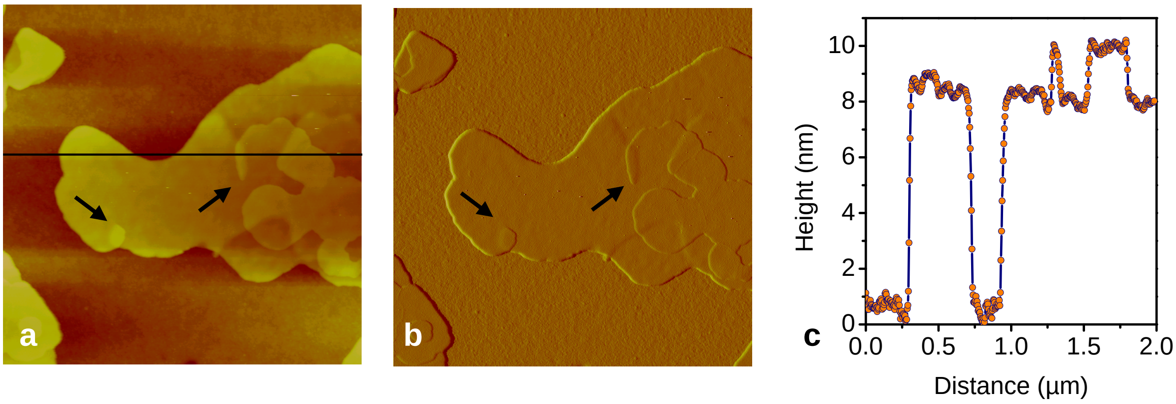

Figure S1 **(a)** Atomic Force Microscopy (AFM) height and **(b)** amplitude image (size 2 x 2 µm^2) of an individual island of compound **2** when vacuum deposited with the substrate held at 140 °C in an area of the substrate that was partially shaded by a clamp during the vacuum deposition. The initial stages of the generation of screw dislocations can be observed (marked by arrows): An advancing front is divided into two traces that form a screw dislocation upon recombination, as described by Schlom et al.[1] **(c)** Height profile at the position indicated by the black line in **(a)**.

[1] D. G. Schlom, D. Anselmetti, J. G. Bednorz, R. F. Broom, A. Catana, T. Frey, C. Gerber, H. J. Guntherodt, H. P. Lang, J. Mannhart, *Z. Phys., B: Cond. Mat.* **1992**, 86, 163

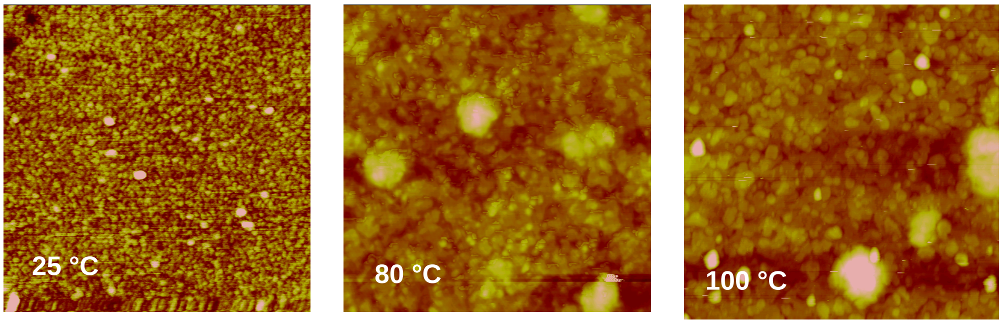

Figure S2 AFM images (2×2 μm^2) of compound **2** deposited at substrate temperatures of 25 °C, 80 °C and 100 °C.

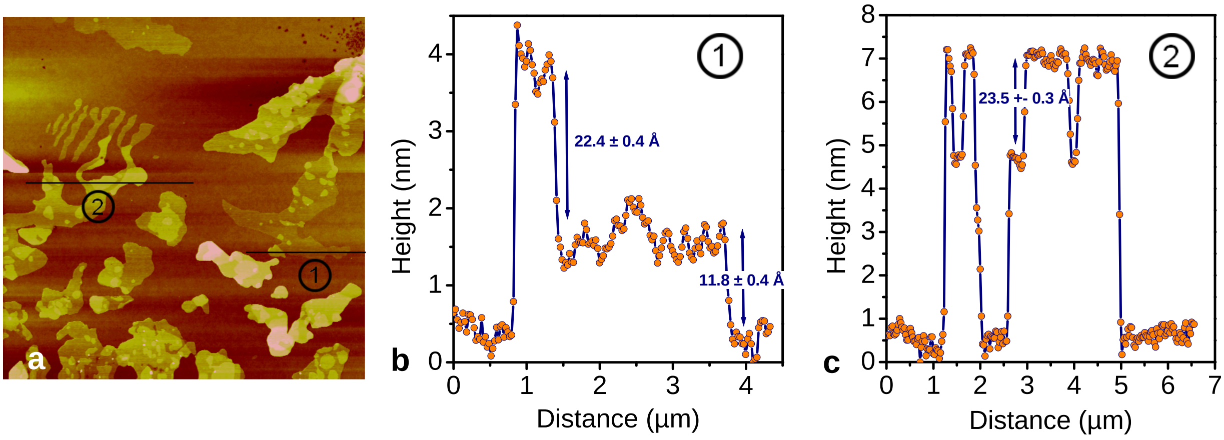

Figure S3 **(a)** AFM image (13.1 x 13.1 μm^2) of a region of the substrate that was partially shaded by a clamp during the vacuum deposition, so that individual islands of compound **2** deposited at a substrate temperature of 140 °C can be observed. **(b)** Scan at position 1 as indicated in **(a).** A step with a step-height of 11.8 Å can be observed suggesting that the molecules are oriented with their long axis parallel to the substrate. **(c)** Scan at position 2 as indicated in **(a)**. The step-height is 23.6 Å.

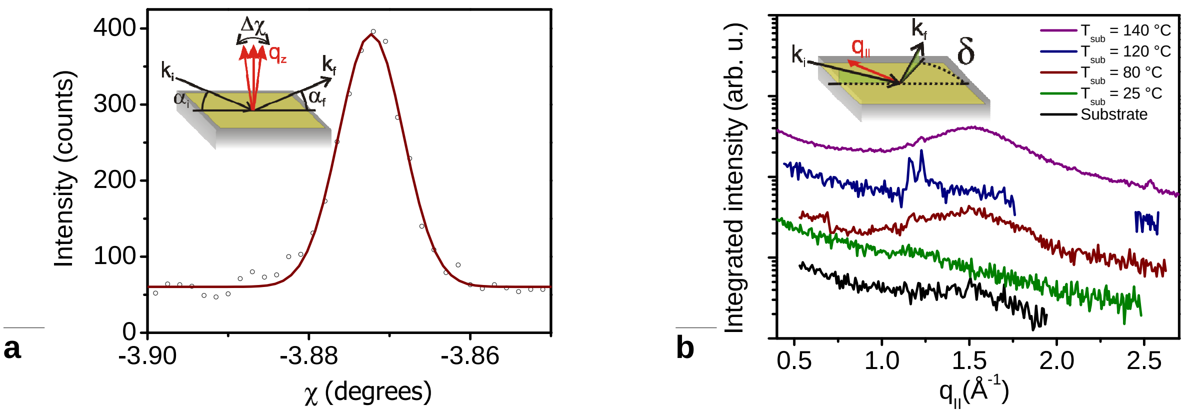

Figure S4 **(a)** Rocking curve obtained for a film of compound **2** deposited at a substrate temperature of 120 °C (q = 0.68342 Å^{-1}). The degree of molecular alignment is excellent, with a mosaicity of 0.008° estimated from the Full Width at Half Maximum (FWHM) of the rocking curves. The data are shown in black, the fit to the data calculated using the Parratt32 software based on the Parratt algorithm is shown in red. **Inset:** Out-of-plane scattering geometry used in the experiment.

(b) Grazing Incidence X-Ray Diffraction (GIXD) data obtained for a film of compound **2** deposited at substrate temperatures of 25, 80, 120 and 140 °C. In-plane reflections observed for the films deposited at 120 °C and 140 °C correspond to an in-plane spacing of 5.39 Å and 5.12 Å, respectively. Note that at a reciprocal wave vector of 2.53 Å^{-1} an in-plane reflection is seen for the 140 °C film, but not for the 120 °C film. In contrast, the reflections at 1.15 Å^{-1} and 1.22 Å^{-1} are observed in both films. This finding supports the hypothesis of the presence of two polymorphs in films deposited at a substrate temperature of 140 °C. **Inset:** In-plane scattering geometry of the experiment.

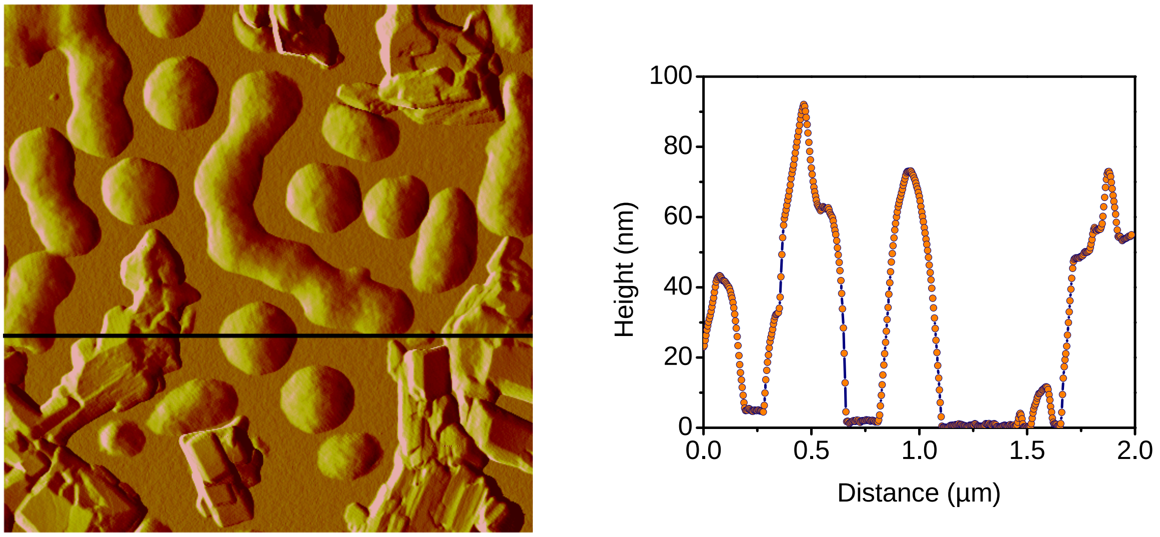

Figure S5: AFM image of compound **1** deposited at a substrate temperature of 100 °C. The film grows in island growth mode. Some islands appear to be amorphous, others appear more ordered with flat terraces. The terraces are not oriented parallel to the substrate. At these high temperatures the molecules seem to have a very low interaction with the underlying substrate and dewet from the surface. Left side: line-scan extracted from the corresponding AFM height image at the position indicated by the black line.

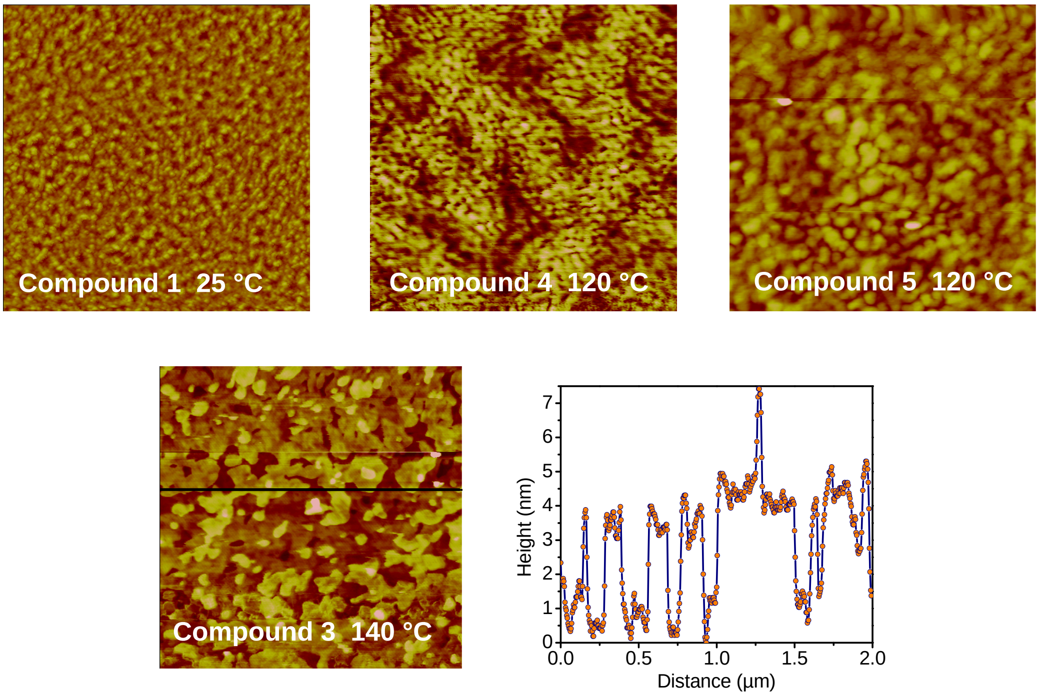

Figure S6: AFM images of compounds **1** and **3-5**. The substrate temperature during the deposition, indicated in each image, is the deposition temperature for which the largest FET mobility was obtained. The line-scan was extracted from the AFM image of compound **3** at the position indicated by the black line.

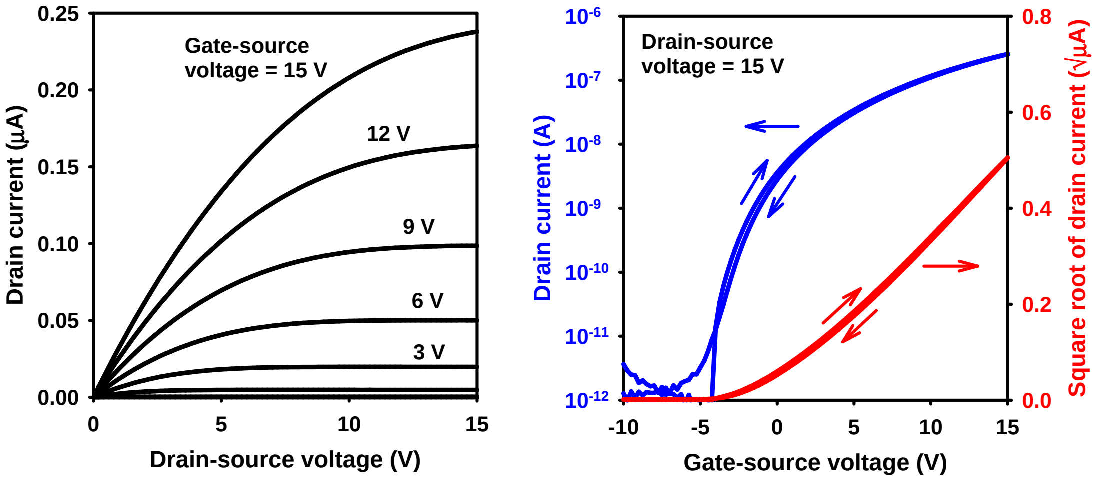

Figure S7 Electrical characteristics of a FET based on compound **3** deposited at a substrate temperature of 140 °C. The transistor has a carrier mobility of 0.05 cm^2/Vs.

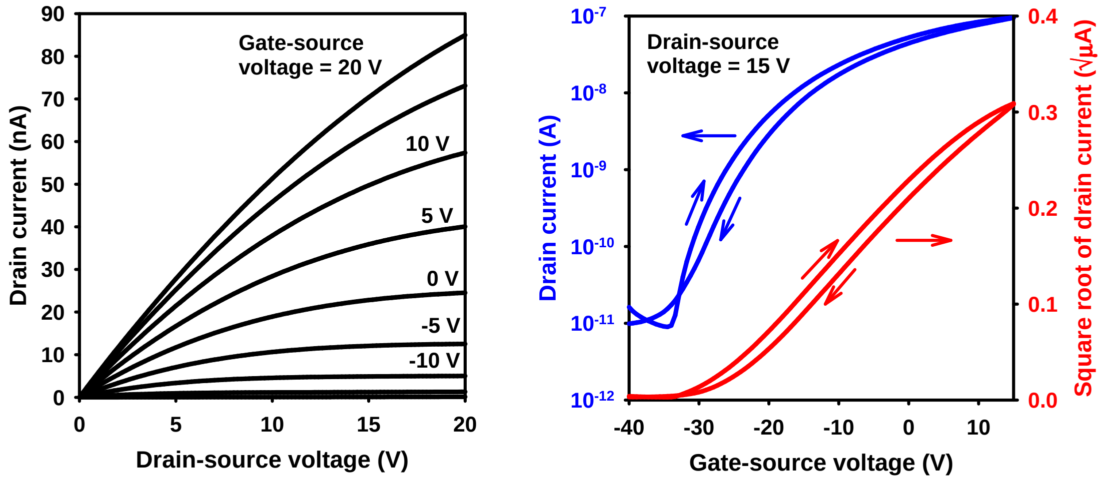

Figure S8. Electrical characteristics of a FET based on compound **4** deposited at a substrate temperature of 120 °C. The transistor has a carrier mobility of 0.004 cm^2/Vs.

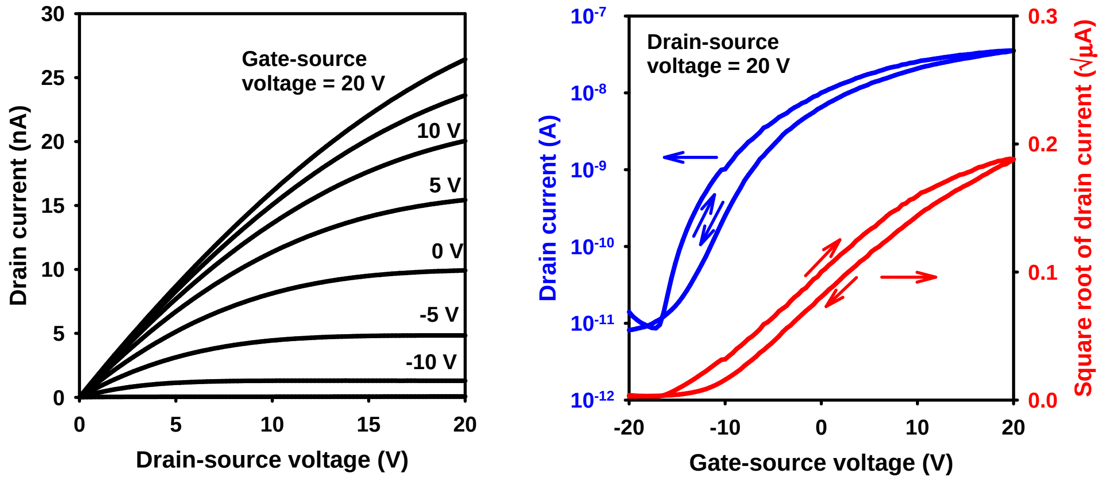

Figure S9. Electrical characteristics of a FET based on compound **5** deposited at a substrate temperature of 120 °C. The transistor has a carrier mobility of 0.002 cm^2/Vs.

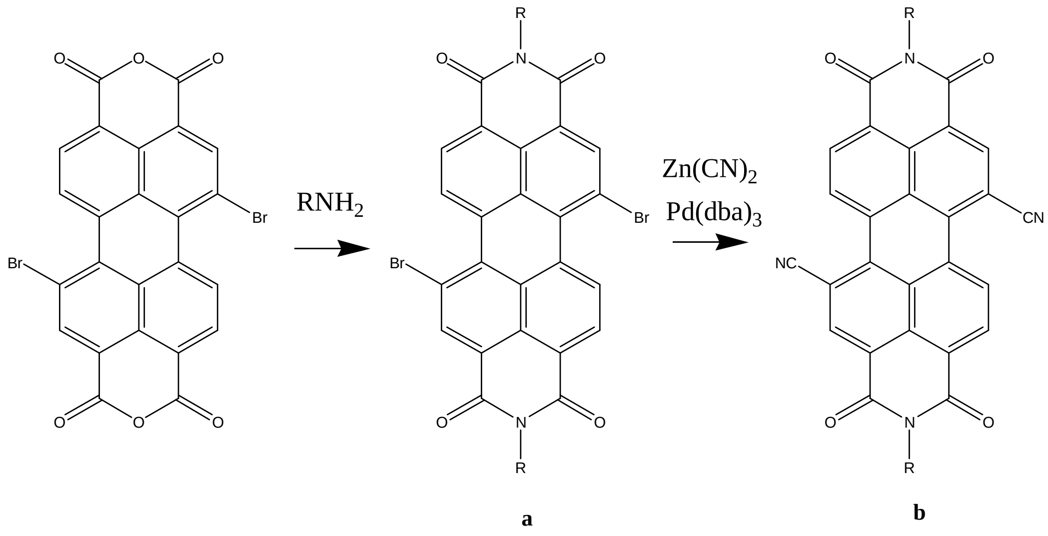

Scheme S1: Synthesis route for compounds **1-5**.

Nuclear Magnetic Resonance (NMR) spectra and Laser Desorption Ionization-Time of Flight Mass Spectrometry (LDI-TOF MS) data of all compounds synthesized in this work are presented on the pages 12-21. All pages are arranged the following way:

(top) NMR spectrum, the number of the compound is indicated at the bottom right of each spectrum. The solvent peak is marked with a *. **(inset)** compound of which the NMR was taken.
(bottom) Experimental LDI-TOF MS spectrum. **(left inset)** calculated MS spectrum **(right inset)** enlarged view of the experimental LDI-TOF MS spectrum.

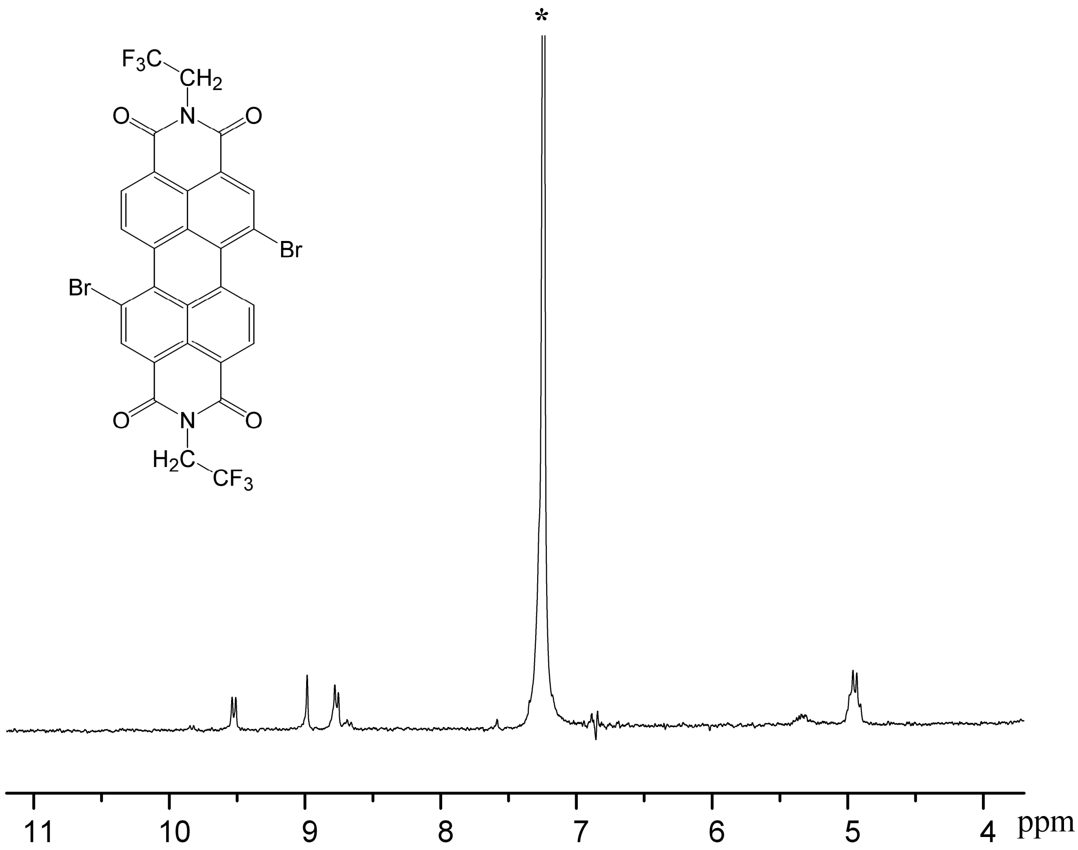

1a. ^{1}H NMR ($CDCl_3$, 300 MHz)

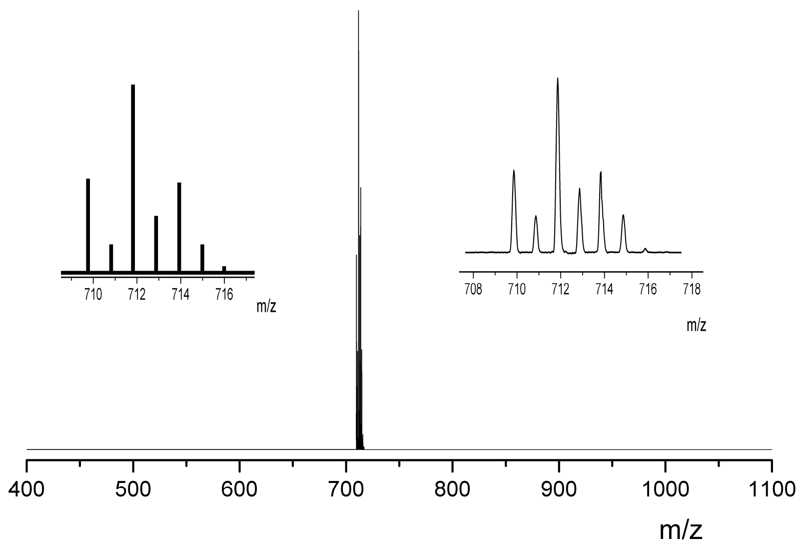

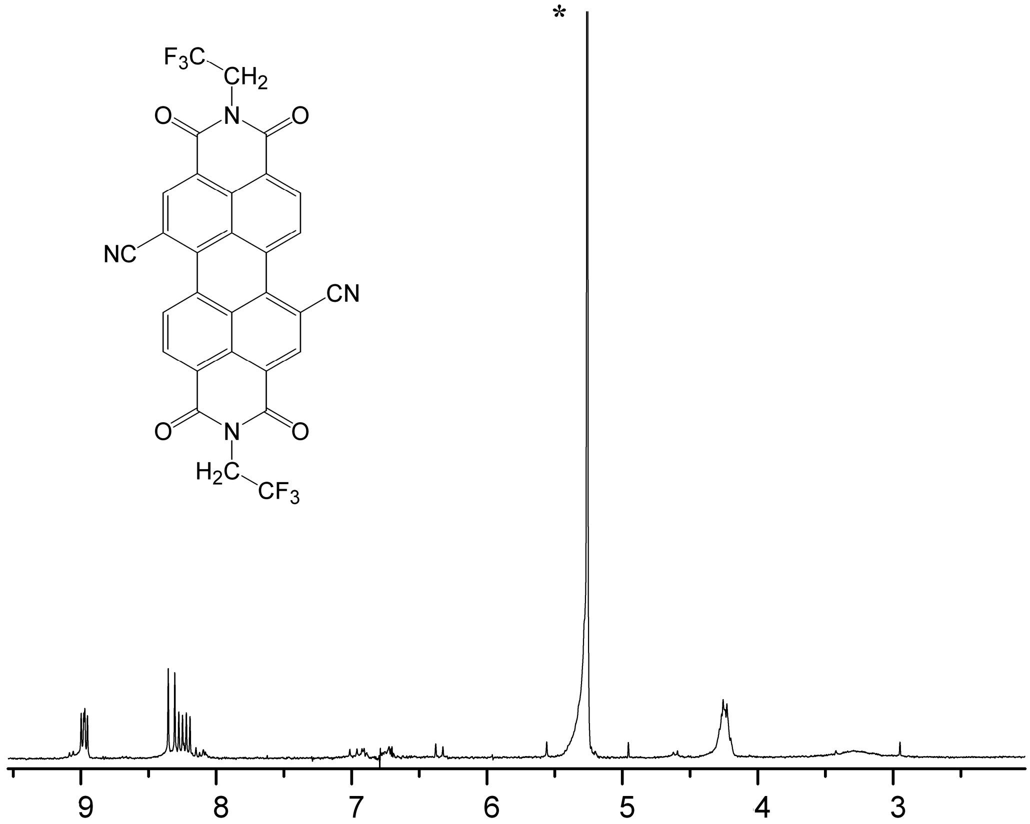

1b. ^{1}H NMR ($C_2D_2Cl_4$, 300 MHz)

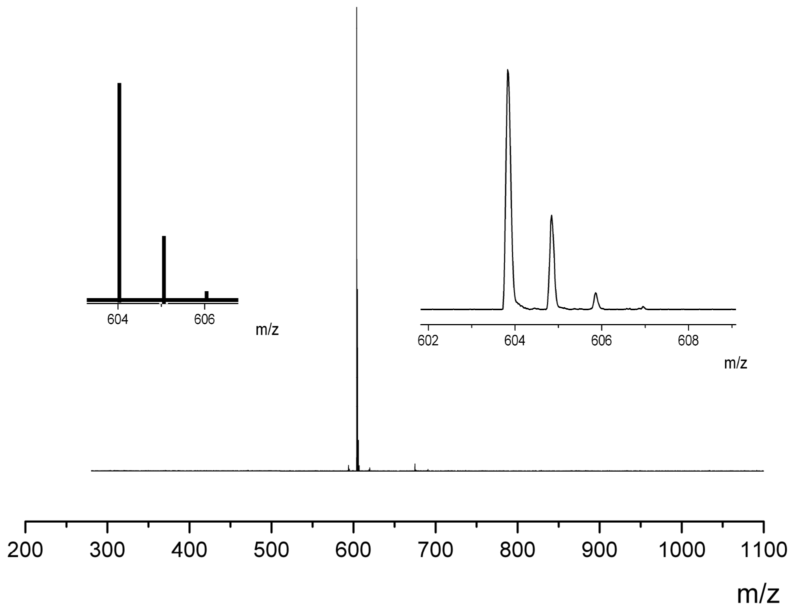

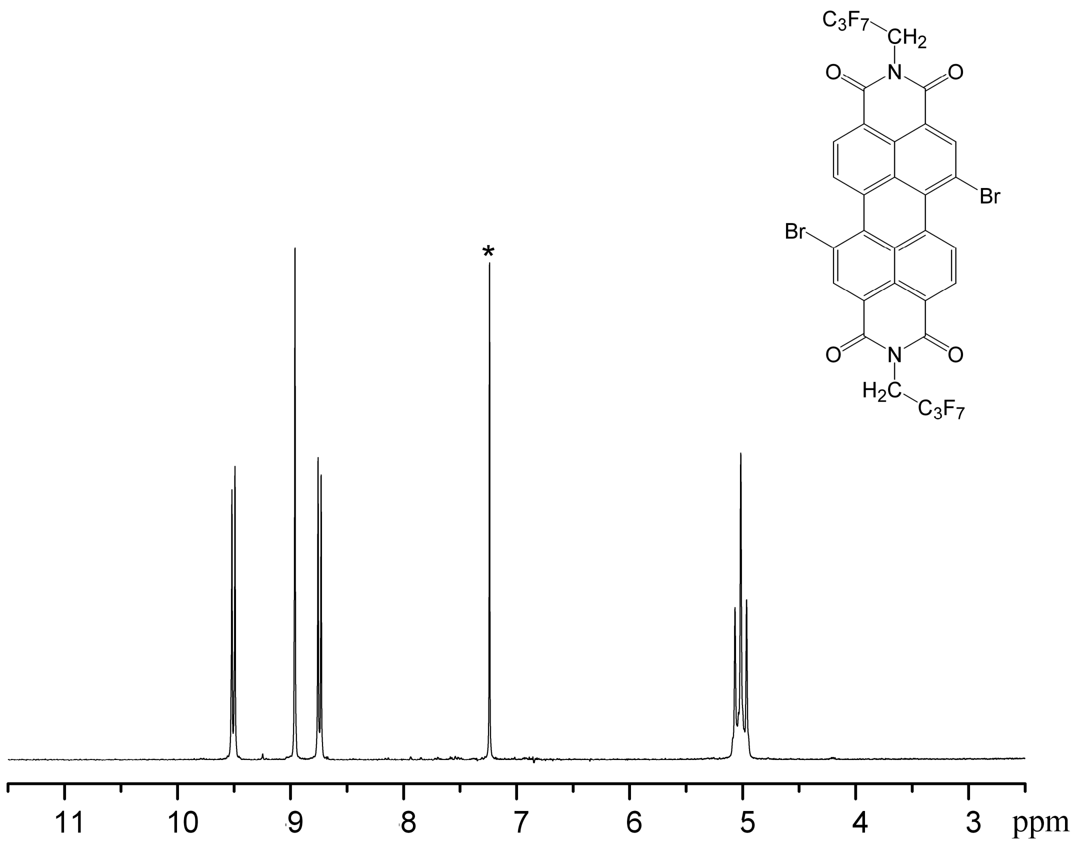

2a. ^{1}H NMR ($CDCl_3$, 300 MHz)

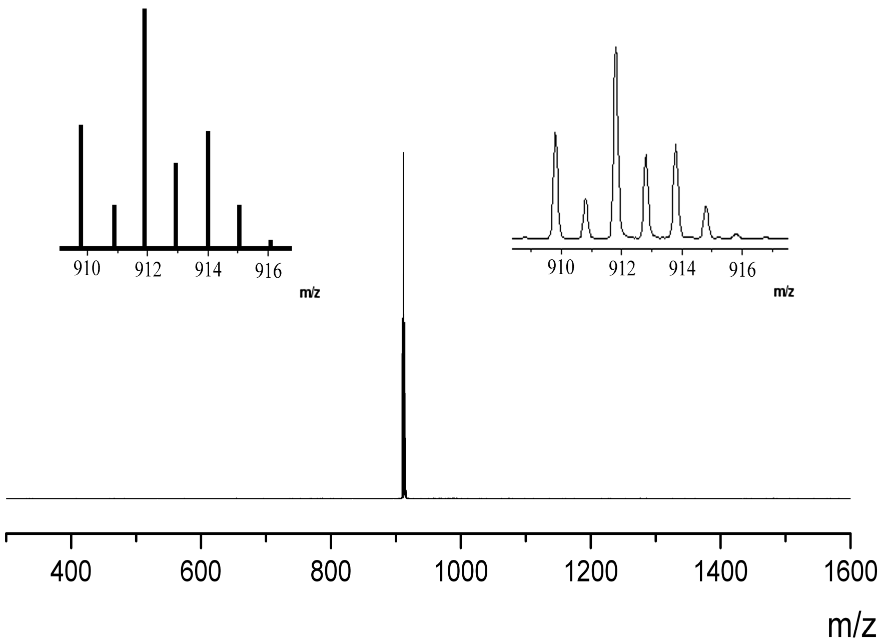

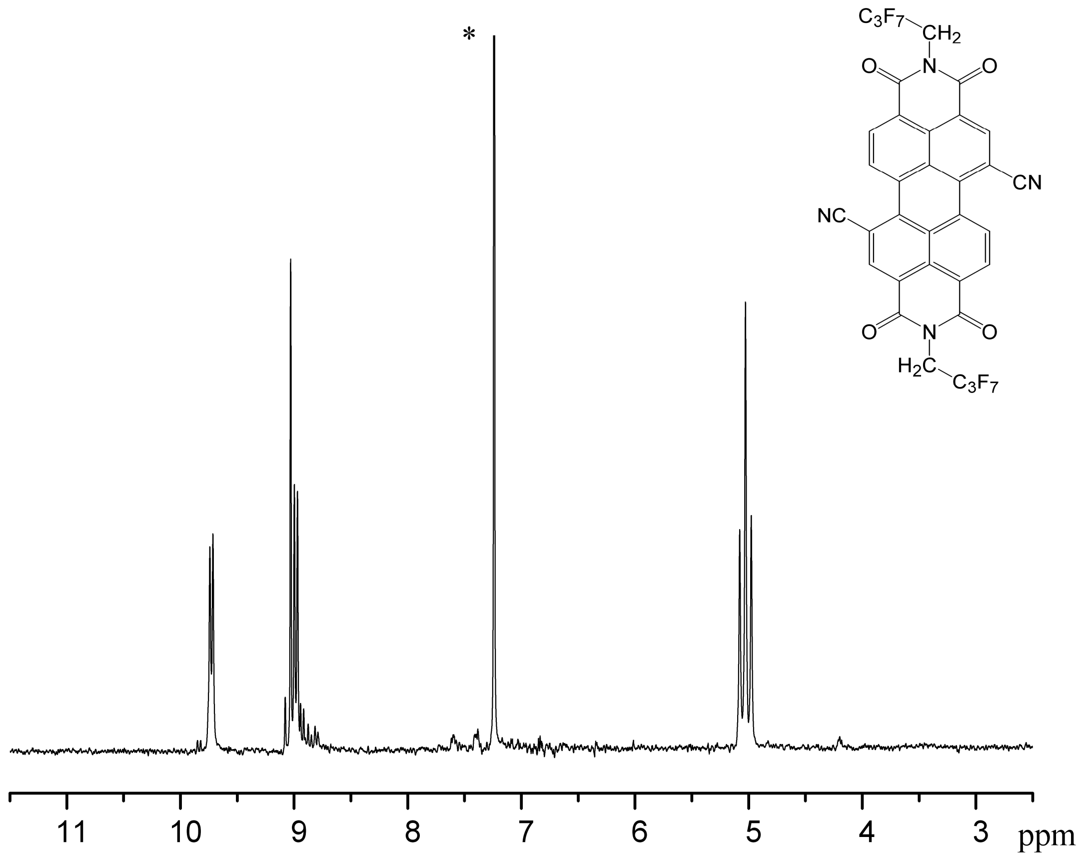

2b. ^{1}H NMR ($CDCl_3$, 300 MHz)

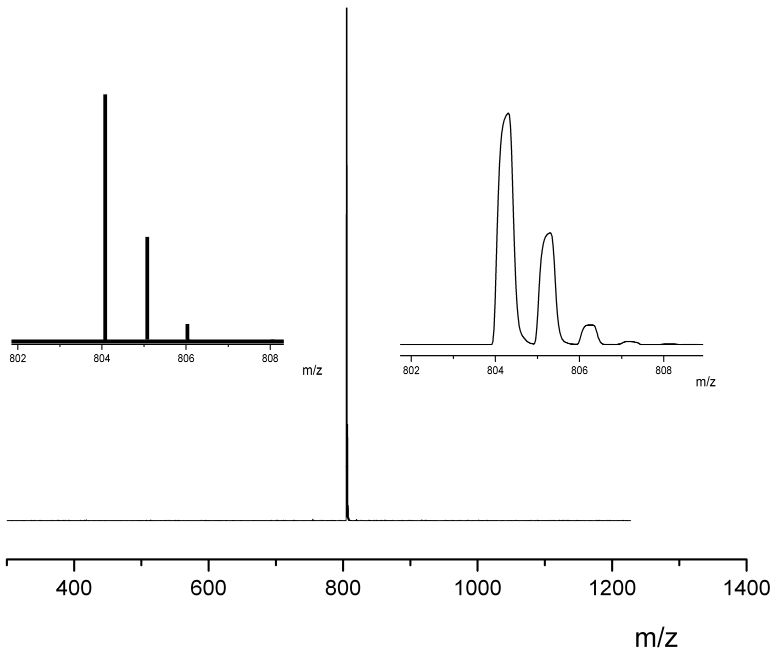

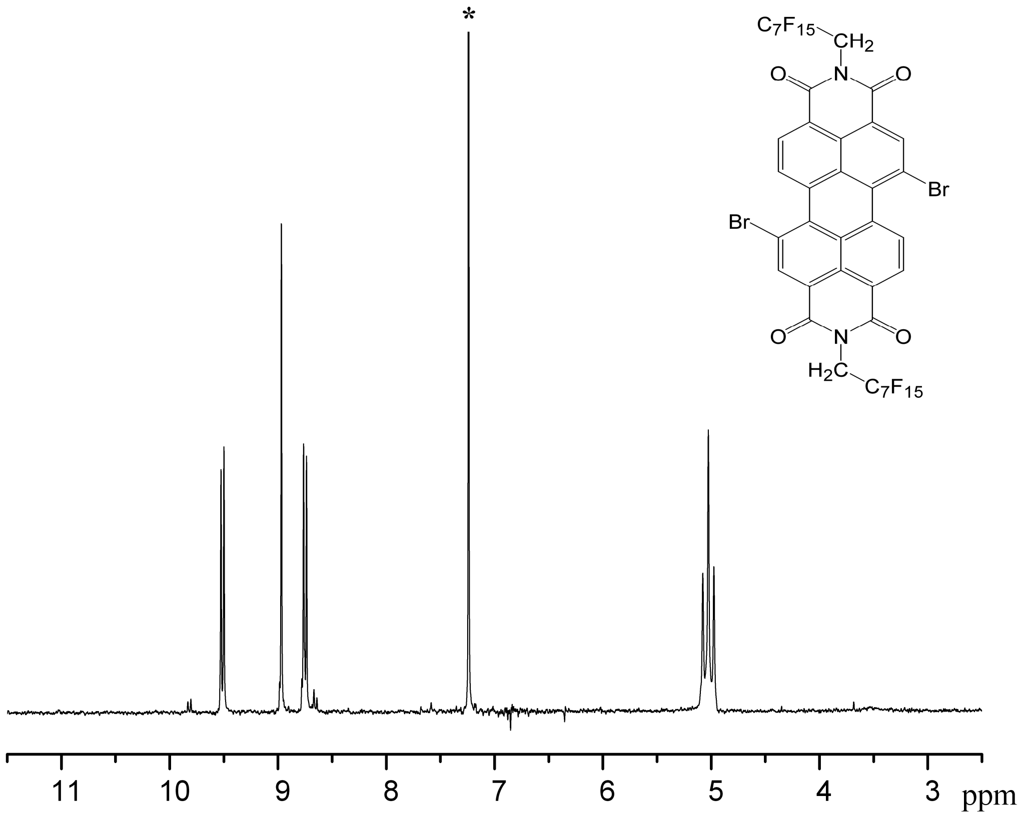

3a. ^1H NMR ($CDCl_3$, 300 MHz)

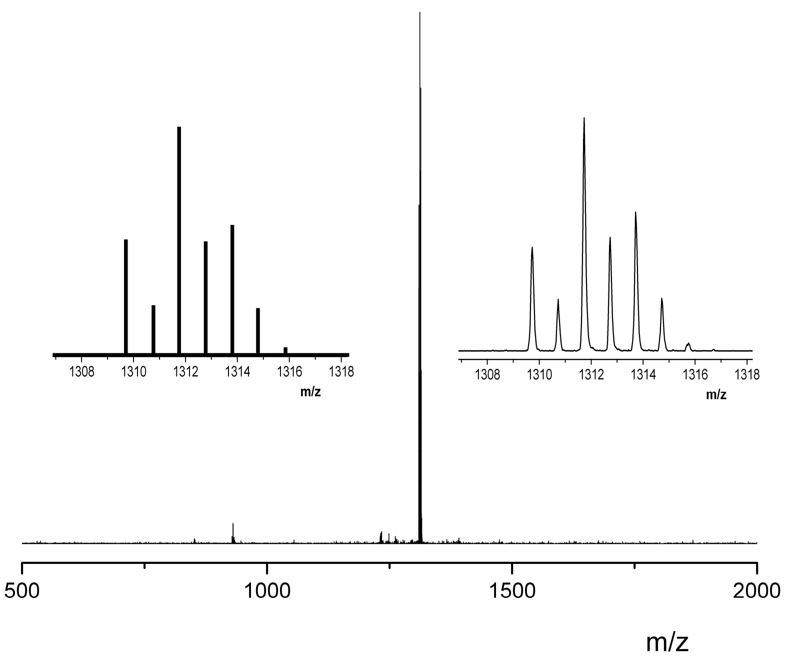

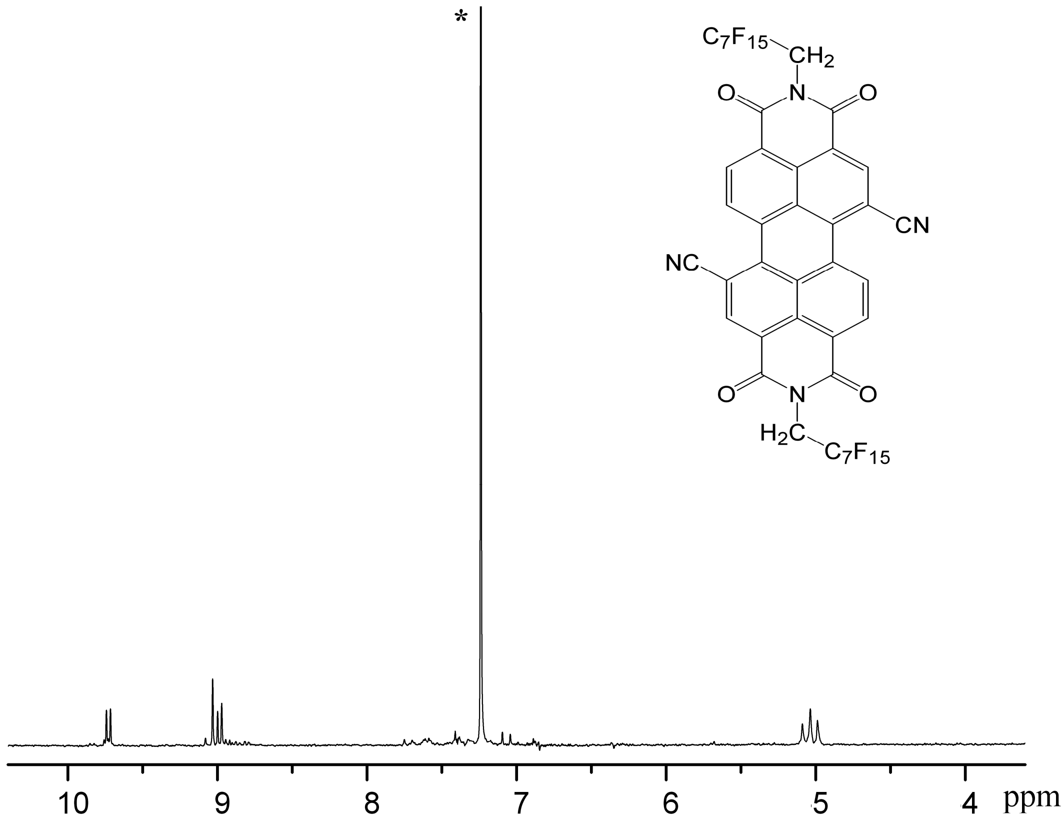

3b. ^{1}H NMR (CDCl$_3$, 300 MHz)

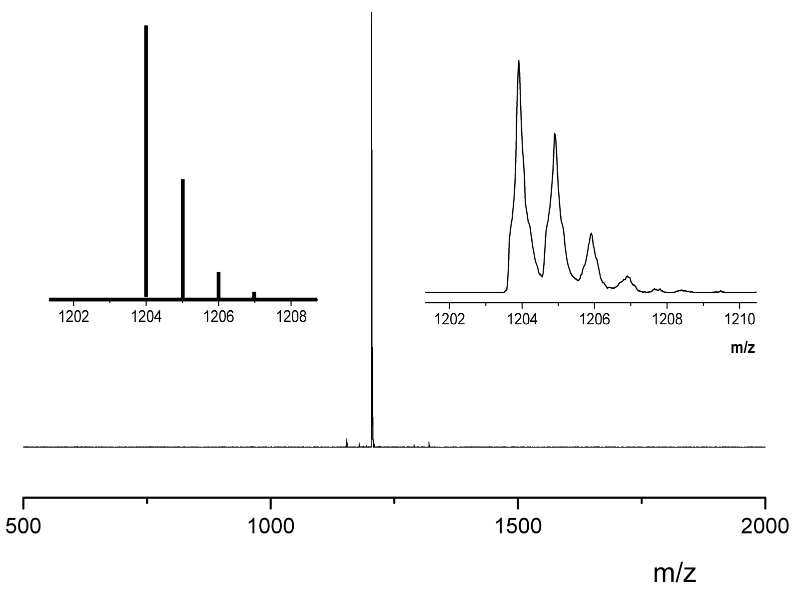

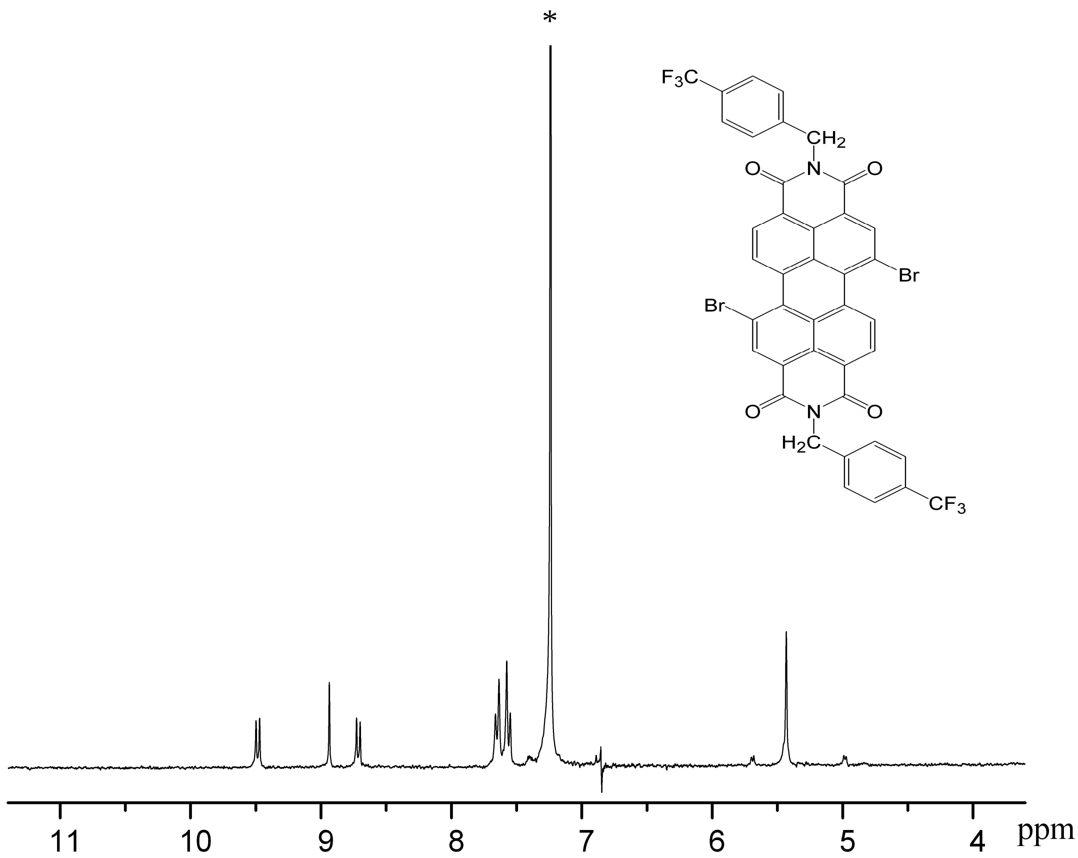

4a. ^{1}H NMR ($CDCl_3$, 300 MHz)

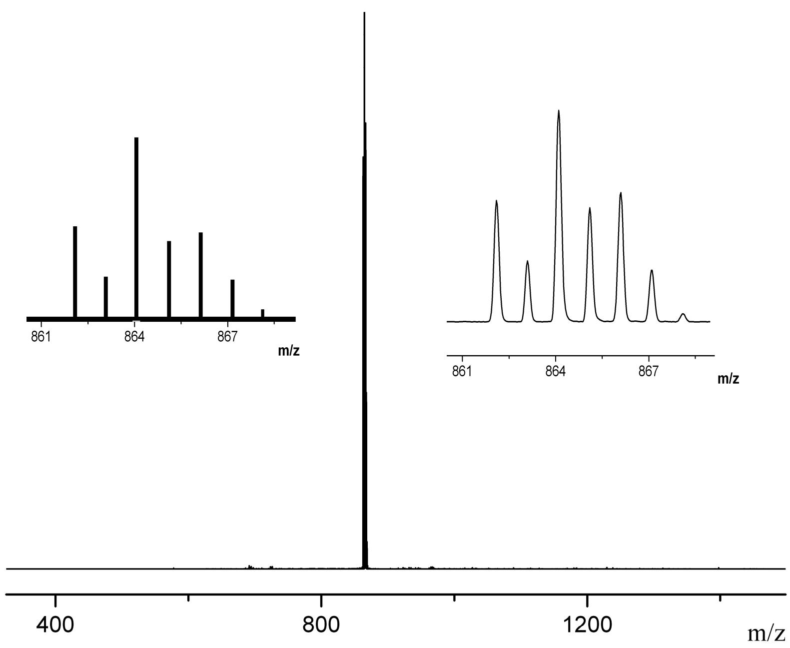

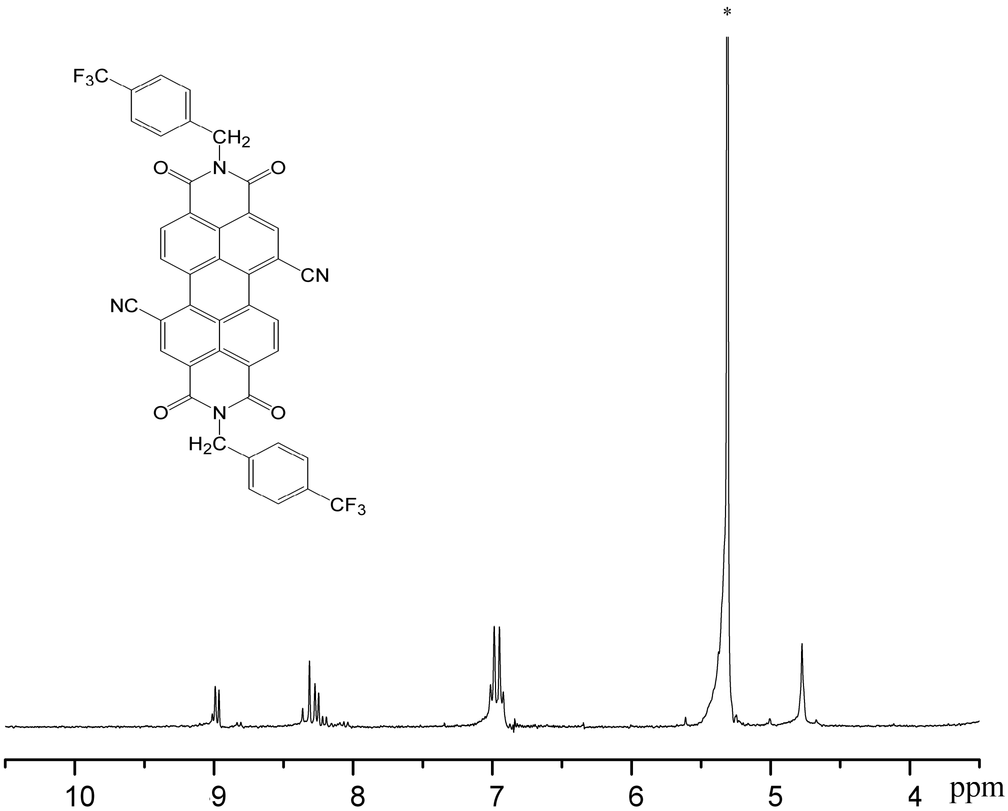

4b. ^{1}H NMR ($C_2D_2Cl_4$, 300 MHz)

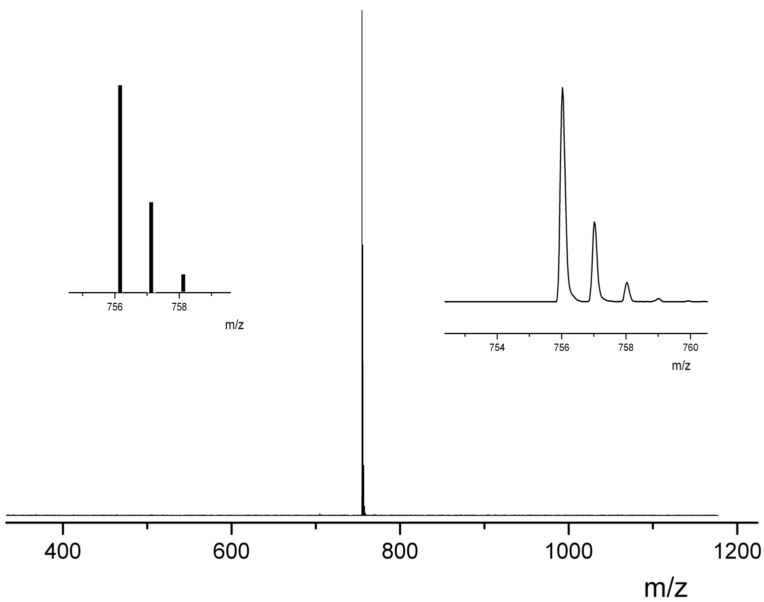

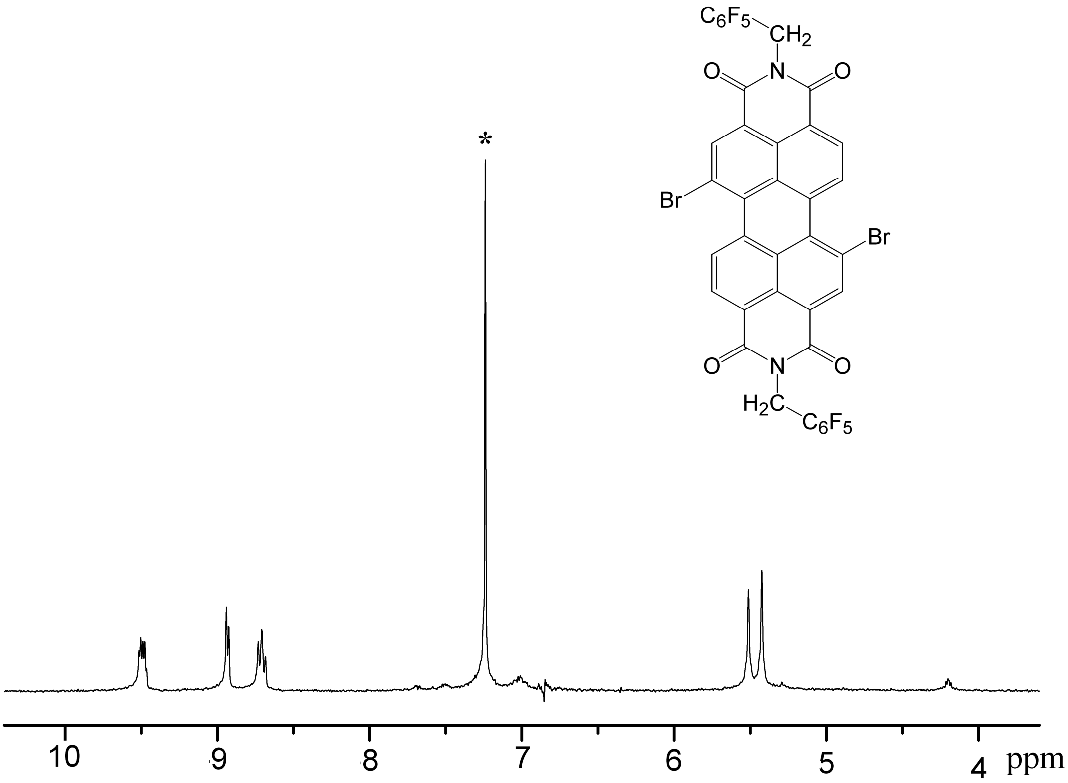

5a. ^1H NMR ($CDCl_3$, 300 MHz)

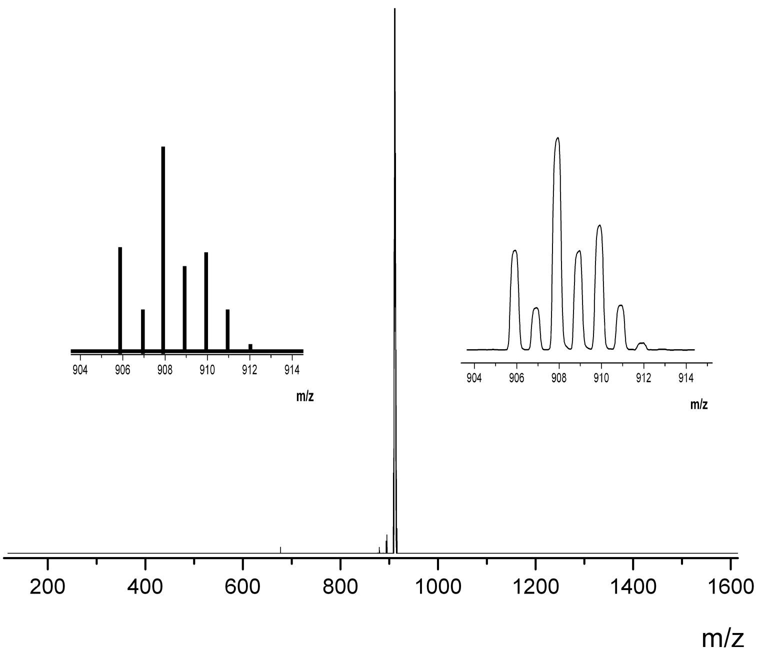

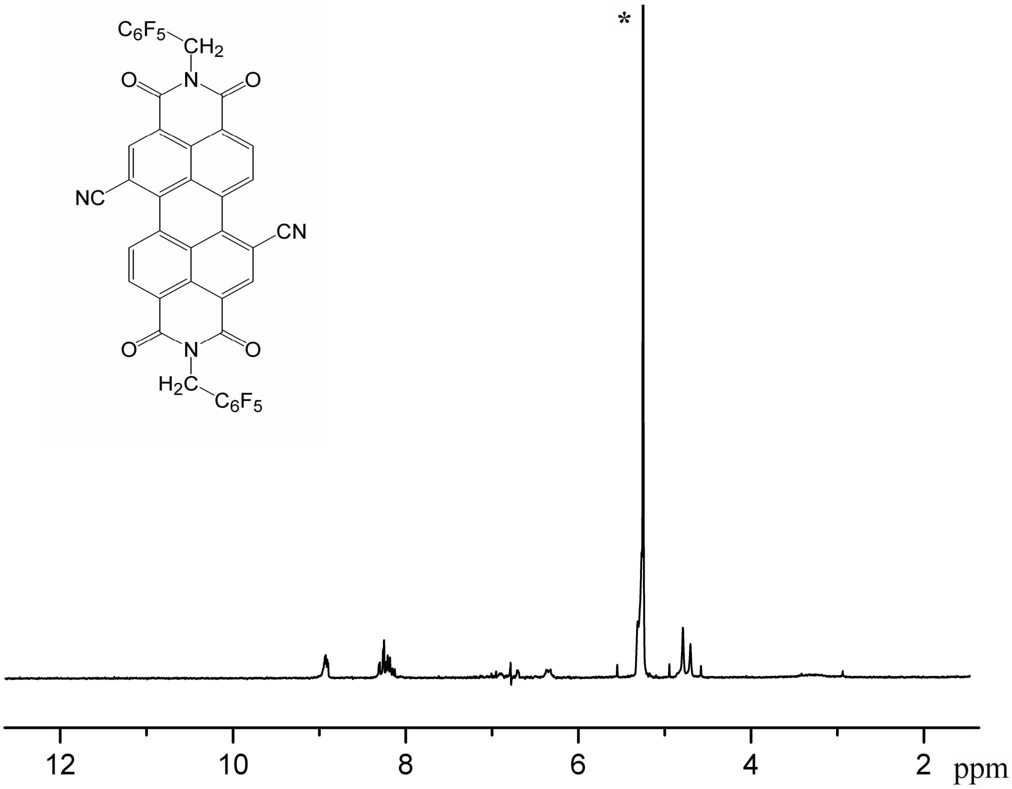

5b. ^{1}H NMR ($C_2D_2Cl_4$, 300 MHz)